DEPARTMENT OF THE NAVY

DAVID TAYLOR MODEL BASIN
WASHINGTON, D.C.

HYDROMECHANICS

o

AERODYNAMICS

o

STRUCTURAL MECHANICS

o

APPLIED MATHEMATICS

o

ACOUSTICS AND VIBRATION

RUDDER-DIVING PLANE-HULL VIBRATION AND FLUTTER ANALYSIS OF USS ALBACORE (AGSS 569)

by

Ralph C. Leibowitz
and
Robert L. Harder

ACOUSTICS AND VIBRATION LABORATORY
RESEARCH AND DEVELOPMENT REPORT

June 1965

Report 1961

RUDDER-DIVING PLANE-HULL VIBRATION AND FLUTTER ANALYSIS OF USS ALBACORE (AGSS 569)

by

Ralph C. Leibowitz
and
Robert L. Harder

June 1965 Report 1961

TABLE OF CONTENTS

TABLE OF CONTENTS
(Continued)

LIST OF FIGURES

LIST OF TABLES

NOTATION

Symbols	Definitions	Unit
$a, \bar{a}, \tilde{a}$	Scale factors (which relate the impedance of the mechanical system to the electrical network) for the hull, rudders, and diving plane	$(\text{ft amp/ton sec volt})^{\frac{1}{2}}$
B	Lift constant for rudder (lift force per unit angle of attack per unit velocity squared)	$\text{ton sec}^2/\text{ft}^2$
b	Vertical distance of the center of mass of the lower rudder below the rudder stock attachment point	ft
b_L	Vertical distance of the center of pressure of the lower rudder below the rudder stock attachment point	ft
C	Damping constant for rudder lateral motion	ton sec/ft
C	Capacitor (subscript indicates mechanical quantity to which it is related)	amp sec/volt
C_c	Critical damping constant for a single degree of freedom system	ton sec ft or ton sec/ft
$\frac{C}{C_c}$	Percent of critical damping	

Symbols	Definitions	Unit
$C_{\dot{y}}$	Pitch damping per velocity, a constant	ton sec^2
c	Damping constant for rudder torsion	ton sec ft
E	Voltage in electrical analog	volt
EI	Bending rigidity	ton ft^2
G	Current per unit input voltage for current generator	amp/volt
GJ_e	Torsional rigidity	ton ft^2
g	Twice the critical damping ratio	
h	Horizontal distance of the center of mass of the lower rudder aft of the rudder stock attachment point	ft
I	Current in electrical analog	amp
I_x, I_z, I_{xz}	Mass moments of inertia of the rudder about its center of mass	ft ton sec^2
I_{mx}	Mass moment of inertia for hull roll motion	ft ton sec^2
K	Scale factor for analog	(ton ft/volt sec amp)$^{\frac{1}{2}}$
K	Radius of gyration for roll of a section of hull mass	ft
KAG	Shear rigidity	ton
L	Inductor for electrical analogy	volt sec/amp

Symbols	Definitions	Unit
L	Horizontal distance of the center of pressure of the lower rudder ahead of the rudder stock attachment point	ft
ℓ	Effective length of rudder stock for computing bending flexibility	ft
ℓ_T	Effective length of rudder stock for computing torsional flexibility	ft
M_y	Mass plus virtual mass for rudder or stabilizer and diving plane lateral motion	ton sec^2/ft
N	Scale factor relating computer time to "real" time. The elapsed time for the actual hull is N times the elapsed time on the computer.	
n	Transformer turns ratio	
$P_{\alpha'}, P_{\gamma'}, \bar{P}_{\alpha'}$ $\bar{P}_{\gamma'}, \tilde{P}_{\beta}$	Scale factors for quantities involving angles. The subscript refers to the angle involved, and the symbol above the P is: none for hull, $\bar{}$ for rudders, and $\sim$ for diving plane and stabilizer.	ft
p, $\bar{p}$	A differential operator, equal to $\frac{d}{dt}$ or $\frac{d}{d\bar{t}}$	1/sec

Symbols	Definitions	Unit
R	Resistor	volt/amp
S	Velocity	ft/sec
S_o	Reference velocity = 84.4 (50 knots)	ft/sec
t, $\bar{t}$	Time, "computer time"	sec
u,v,w	Displacements in x-, y-, and z- directions	ft
x,y,z	Coordinate system (see Figure 1)	ft
$\bar{z}$	Height of center of mass of the hull above the elastic axis	ft
α, β, γ	Rotations about x-, y-, and z- axes, using the right-hand rule (see Figure 1)	
Δx	Length of a section of the hull	ft
μ	Mass of hull per unit length	ton sec^2/ft^2
ν	Poisson's ratio	

Note: A dot above a symbol represents differentiation with respect to time.

ABSTRACT

This report presents the results of a "flutter" analysis for the submarine USS ALBACORE (AGSS 569). The results were obtained both by performing a simple control-surface computation using analytical expressions derived in this report and by computing the rudder-diving plane (and stabilizer) - hull vibrations (including flutter) on an analog computer. The analogs are based upon previously derived theories and methods for representing the vibrating system and for evaluating the control surface-hull parameters referenced in this report.

The analytical and analog results are in excellent agreement and indicate that control-surface flutter of ALBACORE will occur at about 90 knots.

INTRODUCTION

It seems certain that as ship speeds increase, hydroelastic interactions will produce classical control-surface and/or subcritical flutter* within the operating speed range. For evidence favoring this cogent assertion, witness:

1. The severe vibrations transmitted to the hull of USS FORREST SHERMAN (DD 931) by the rudder during a steady horizontal turn.[1,2]

2. The occurrence of classical flutter for two different types of models tested in the TMB towing basin.[3,4]

Thus, development of methods for making accurate control-surface flutter predictions on high-speed ships (including hydrocraft) is presently of consequence in anticipation of the probable near-future needs of the ship designer to prevent flutter and/or excessive vibrations.** How then can the designer perform a flutter analysis for real ships? The answer to this question, which is the primary objective of this report, will be given by way of a specific application of this analysis to USS ALBACORE (AGSS 569). This ship was chosen for computational convenience; it is the only ship for which essentially all of the theoretical and experimental data for the control surface-hull system, necessary for computation, were readily available.[5,6,7] The computation is intended only as an illustration of an

*Classical flutter is a dynamically unstable, self-executed vibration of an oscillatory system immersed in a field of fluid flow. Subcritical flutter is a condition of barely stable vibration due to marked reductions in the overall damping of the system.

**For example, to forestall possible undesirable vibration characteristics or flutter, the Bureau of Ships recently requested the author to perform a flutter analysis for PGM Motor Gunboat. (BuShips ltr PGM/9400 Ser 442/235 of 4 Jun 1963.) This will be the subject of a future report. (See RECOMMENDATIONS).

application of the *procedure* for making control surface-hull calculations.* This will provide the designer with a concrete guide for making similar computations for more realistic applications (i.e., higher speed ships) and also for extending or modifying the present procedure, if necessary.

In Reference 8, a theory for computing rudder-diving plane-ship vibrations including flutter on a digital and/or analog computer was devised.** Application of this theory requires an evaluation of the physical and hydroelastic parameters for the hull-control surface system for use as coefficients in the differential equations of motion of the system. The method for evaluating the physical (mass-elastic) parameters for the hull is given in Reference 11 and for the control surfaces† in References 6 and 7. The method for evaluating the hydroelastic parameters for the control surfaces is given in Reference 5. Based upon the equations, computational procedures, analogs, and

*It is stressed that for the prediction of flutter speed the authors have proved that which was fairly obvious to them prior to making the computation; namely, that ALBACORE control surface would only flutter at some very high speed (the calculations predicted the specific speed to be 90 knots). The chief objective of this report, however, is to illustrate a method for application to other ships for which flutter might occur within their operating speed ranges. Thus, the method is intended to be of use in the design of ships other than ALBACORE.

**The relatively simple representation for the hydrodynamic loads used in this theory are based upon the Modified Theodorsen Analysis discussed in References 9 and 10. Comparison of predicted and observed values of (1) damping and (2) critical flutter speeds made in Reference 10 shows that the results of this analysis are in good agreement with experimental data. Thus, the theory was considered adequate for the present problem (see RECOMMENDATIONS).

†Actually, only rudder parameters were given in References 5 and 6. Parameters for the diving planes (and stabilizers) are similarly treated in the present report. The damping parameters for the rudder are discussed in detail in Reference 7 and cryptically in Reference 5.

control surface-hull data (Table 1 of Reference 5 presents these data for ALBACORE) given in these references, a flutter computation for ALBACORE is made in the present report by means of an electric-analog computer.* The results of this computation are the natural frequencies, mode shapes, critical flutter speeds, and damping of the control surface-hull system and/or parts of this system as well as certain other data of interest. In addition, an analytical method of solution for the flutter of a cantilevered control surface is devised and used to determine the flutter speed and frequency of the rudder, for comparison with the values determined by the analog computer.

*The flutter computation can also be made on a digital computer (see RECOMMENDATIONS).

THEORETICAL ANALYSIS OF THE PROBLEM AND METHOD OF ATTACK

The solutions for the normal modes and flutter of a combined rudder-diving plane-hull system in forward motion and subject to hydrodynamic forces are based upon the theory derived in Reference 8. In this reference the control surfaces were treated as rigid bodies attached through flexible stocks to a flexible hull, and small vibration theory was assumed to be applicable; the validity of treating such control surfaces as rigid bodies was experimentally demonstrated in Reference 6. The procedure requires evaluation of the inertias, elastic constants, and hydroelastic parameters of the system. The method of evaluation of the parameters associated with the equations of motion for a vibrating hull alone is described in Reference 11 and the computation of hull parameters for ALBACORE was made in Reference 5. The inertia-elastic and hydroelastic constants for the rudders of ALBACORE were computed in References 6 and 5, respectively.* In the present report the diving plane (and stabilizer) system is simplified to represent ship plans for ALBACORE. The elastic and hydroelastic constants for this simpler model were computed using these plans.

The actual solutions for the natural frequencies, mode shapes, critical flutter speeds, and damping of the system and/or parts of the system were obtained by means of electrical analogs which represent the equations of motion of the combined or partial system.** The mechanical system modeled by these analogs and the source of

*These constants are associated with Equations [62a], [62b], and [62c] of Reference 8 for the motions of the rudder alone. Page 2 of Reference 5 discusses these parameters in greater detail.

**Solutions can also be obtained by use of a digital computer.[8]

these analogs are discussed as follows:

1. For the inertial-elastic hull undergoing torsion-horizontal bending vibrations, the analog given in Figure 26 of Reference 11 was used. The general circuit presented there, however, was simplified to omit certain terms not pertinent to the present analysis.

2. For interpolation of the rudder connection to the hull, the analog given in Figure 9 of Reference 8 was used.

3. For the rudder system (rigid rudder-flexible rudder stock) undergoing transverse vibrations, the analog given in Figure 8-I of Reference 8 was used.

4. For the hydroelastic forces on the rudder, the analog given in Figure 28 of Reference 8 was used.

5. For the diving plane and stabilizer system, the inertial and hydroelastic analogs are developed in this report; see Appendix A.

The actual electrical analogs used for the solution of ALBACORE motions and certain details pertinent to their development are given in Appendix A.

DESCRIPTION OF HULL-RUDDER-DIVING PLANE (AND STABILIZER) SYSTEM

Figure 1 shows the major components of the submarine system consisting of the hull and sail,* two rudders, and two stabilizer-diving planes. With respect to the coordinate system shown in the figure, the submarine hull and appendages are symmetric about the x-z plane through the center of the ship and only antisymmetric motions about

*The sail is not included in the analysis.

this plane are treated; see Appendix B. Thus, due to symmetry, the complete masses and stiffnesses of the hull are used; however, since only one diving plane is included, twice its mass and spring constant is used.

THE HULL

The hull is treated as a 20-cell beam with bending and shearing flexibility and a 20-cell torsion bar[12]* with torsional inertia and mass coupling. Hull parameters are given in Table 1.** The hull is free to move laterally along the y-axis, yaw (γ) about the z-axis, and roll (α) about the x-axis.

For the *basic* case, bending and torsion of the beam are uncoupled unless the upper and lower rudder systems are asymmetrical. To represent and evaluate this effect, a mass coupling was arbitrarily added by assuming that the location of the center of mass was at a location $\bar{z}$ of 0.2 x radius above the elastic axis of the hull (see Table 1). The elastic axis was taken to be at the centerline of the hull. With $\bar{z}$ included, the mass ($\mu\Delta x$) and torsional inertia (I_{mx}) about the elastic axis are left unchanged.

THE RUDDERS

The rudder is treated as a rigid planar body flexibly attached to the hull by a beam-torsion bar,[12]* as shown in Figure 2. This figure also gives the values of the rudder parameters for the basic configuration.

*A 20-cell torsion bar is a bar in which the continuous rotary inertia properties have been lumped into 20 discrete rotary inertia elements and the continuous torsional flexibility properties have been lumped into 19 discrete flexibility elements which alternate with the inertia elements. Reference 12 describes the process by which a *torsion rod* is lumped into discrete elements and gives the development of the equivalent electrical circuit. This reference also gives similar information for a beam with inertially coupled bending and torsion characteristics (beam-torsion bar). The circuit of Reference 12 may be compared with the circuit presented in this report (see Figure 21).

**The method for evaluating hull parameters is described in Reference 11; for ALBACORE hull parameters, see Table 1 of Reference 5.

THE STABILIZER-DIVING PLANE SYSTEM

The stabilizer is treated as a one-cell beam without shear or torsion flexibility. The diving plane is treated as a rigid planar body which is supported at both ends by the stabilizer and constrained in β motion by a torsion spring. Figure 3 shows the geometry of the starboard diving plane-stabilizer system and the values of the parameters for this system.

The torsional constraint for the stabilizer means that the rotation angle β for the stabilizer does not exist. Hence, hydrodynamic forces arise only from the angle β of the diving plane and the plunge $\dot{z}$ of the diving plane and stabilizer. For x-y-γ motion, the stabilizer-diving plane system is assumed to be rigid and the masses lumped into the hull.

ANALOG RESULTS

MODES

Normal modes* of the submarine hull and its appendages, including virtual mass, observed on the analog computer, are presented in three forms:

1. Plot of the node lines for the cantilevered rudder (those points which have zero y motion).

2. Tables of frequencies, mode shapes, and computer parasitic damping.

*These modes correspond to the natural frequencies of the undamped system. Modes are found by driving some *electrical* node (point on the structure) with a voltage of constant amplitude (velocity) and observing those frequencies for which the current (force) is a minimum. Usually several nodes are tried to be sure that all frequencies are found. At each frequency the voltage is fixed (usually at the point of largest voltage), and the parasitic damping g is measured by the "3-db method" (see Appendix C).

3. Plots of hull deflection and twist.

Linear dimensions are given in feet, angles in radians, and frequencies in cycles per minute. Only antisymmetric modes about the vertical plane of symmetry are treated.

Modes of the Cantilevered Rudder

Table 2.1 shows all the mode shapes and frequencies of the cantilevered rudder represented as an idealized structure with only three degrees of freedom. These frequencies are also presented in Table 2.4. The amplitudes have been normalized so that y-deflection of the center of mass is 1 in. The analog results are compared with the digital results obtained in Reference 6.

Figure 4 is a plot of the node lines for the rudder showing the locations of the center of mass and pressure and the bending center.*

Modes of the Cantilevered Stabilizer-Diving Plane

Table 2.2 shows all the mode shapes and frequencies of the horizontal surfaces represented as an idealized structure with only two degrees of freedom.

*The bending center is defined to be that point for which a unit static force in the y-direction would produce no rotations of the rudder, and it is at the "center of gravity of the 1/EI diagram" for the rudder stock. This definition, for a cantilevered rudder, assumes the hull is rigid and clamped. The rudder stock bends laterally as a beam cantilevered below a certain point at which it is effectively clamped to the hull--the center of gravity of the 1/EI diagram of the rudder stock. Zero elastic coupling (due to the stock) between rudder roll and yaw causes the bending center, as defined above, to be located on the rudder stock centerline.

In this analysis, the rudder stock bending flexibility was assumed to be uniform (EI constant) over its entire effective bending length $\ell = 4.167$ ft, from the point at which it is attached (cantilevered) to the hull to the point at which it is attached to the rudder. Thus the "bending center" is at the midpoint of the stock indicated in Figure 2. This point is 5.00 ft below the hull centerline, and is indicated in Figure 4.

In the lumped model of the structure, a Russell bending cell[18] is employed in the analogy, and the single lateral bending spring representing the bending flexibility of the rudder stock is located at this bending center.

Modes of the Hull

Table 2.3 compares the hull mode frequencies found on the analog computer with those given in Reference 6 for horizontal bending only (no appendages considered). Table 2.4 also gives the first two torsion frequencies of the hull. Also, there are three zero frequency, antisymmetric modes (unlisted); namely, lateral translation, yaw (rigid γ rotation), and roll (rigid α rotation). Figures 5.1 and 5.2 show the first two finite frequency bending modes and Figure 5.3 shows the first torsion mode for the hull.

Hull with Rigid Appendages

Table 2.4 and Figures 5.4-5.8 show the nonzero frequencies and modes of the hull with rigid appendages.

Hull with Flexible Appendages

Table 2.4 and Figures 5.9-5.15 show the nonzero frequencies and modes of the hull with flexible appendages.

Hull Mode Frequencies Including Mass Coupling

Table 2.5 shows the hull mode frequencies of the hull with mass coupling.

FLUTTER

In this analysis, all velocities are given in terms of S/S_o, S_o being a reference velocity of 50 knots (84.4 ft/sec). Damping is given in terms of g, which is twice the critical damping in percent.* Basic values of the hull and rudders are presented except where otherwise stated. In several cases, data are presented as amplitude versus frequency plots on logarithmic coordinates. Appendix D explains how to read these plots.

*Appendix C describes the method used to measure g.

Rudder Damping versus Velocity; C = c = 0: L Variable

Figure 6 shows a plot of rudder damping versus velocity for C = c = 0 and various values of L. Results for both the cantilevered rudder and rudders attached to the hull are given.

Frequency and Damping of Cantilevered Rudder versus Velocity; C = c = 0

Figure 7 is a plot of the variations of the three modes of the cantilevered rudder over the velocity range of interest.

Amplitude versus Frequency of (a) Cantilevered Rudder, (b) Rudder Attached to Hull, and (c) Hull;* L = 0

Figure 8.1-8.5 are plots of the cantilevered rudder amplitude γ versus frequency, over a range of velocities and at zero damping, for a force of constant amplitude α applied at the center of pressure of the rudders. Figures 8.6-8.10 and 8.11-8.15 are similar plots for amplitudes of the rudder γ and hull at Station 1.5 y, respectively, when the hull is included. Figures 8.16-8.21 and 8.22-8.26 show plots for amplitudes of the hull at Station 1.5 (y) and rudder (γ), respectively, when the hull is included but damping is not zero; Figures 8.27-8.31, for the amplitude of the hull (y) at Station 18.5, where the rudders are attached, when the hull is included.

Amplitude versus Frequency of Hull;** L = ±

Figures 9 and 10 are plots of the amplitude of the hull (y), at Station 1.5, versus frequency, over a range of velocities and with positive damping, for a force of constant amplitude applied at the center of pressure of the rudders and for L = 0.9 and -0.3, respectively.

*In (c) the hull is with rudders attached.
**With rudders attached.

Amplitude versus Frequency of Cantilevered Stabilizer and Diving Plane

Figure 11 is a plot of the amplitude of the diving plane rotation angle (β) versus frequency for the cantilevered stabilizer-diving plane system, over a range of velocities and with positive damping, for a force of constant amplitude applied at the center of pressure of the diving plane.

Amplitude versus Frequency of the Basic Submarine and Its Modifications

Figure 12 plots the amplitudes of the motions of the rudder and hull versus frequency, over a range of velocities and with positive damping, for a force of constant amplitude applied at the center of pressure of the lower rudder only. Figure 13 is a similar plot* except that the rudder and diving plane flexibilities have been increased by a factor of 4. Figure 14 is also similar except that mass coupling has been added to the basic hull (i.e., the center of mass has been placed above the elastic axis of the hull a distance $\bar{z}$ as shown in Table 1).

Dynamic Stability Plots for Cantilevered Rudder; h Variable

Figure 15.1 shows rudder damping versus velocity for several values of h (center of mass). Figure 15.2 plots critical velocity versus h. Both plots are for cantilevered rudder.

Damping versus Velocity of Cantilevered Rudder; h and L Variable

Figure 16 plots rudder damping versus velocity for several combinations of h and L of the cantilevered rudder.

*Due to a change of time scale factor, the frequency scale on the chart has changed for this case.

Amplitude and Phase Response of Basic Submarine with Mass-Coupled Hull

Figure 17 shows a complete record of the response of the submarine with a mass-coupled hull. The amplitude and phase of all motions have been recorded at five velocities and at the frequency for which the rudder amplitude is greatest. The phase given is in degrees of lag behind the force on the lower rudder and is the phase of the velocity or force.

Rudder Pitch Damping versus Velocity for a Cantilevered Rudder

Figure 18 shows, for the cantilevered rudder, a plot of the rudder pitch damping versus velocity for several values of yaw damping.

Amplitude versus Frequency of Basic Submarine

Figure 19 plots the motions of the rudder and hull and the forces and torques on the hull versus frequency, over a range of velocities and with positive damping, for a force applied at the center of pressure of the lower rudder only. Figures 19.1-19.3 and 19.10-19.15 apply to the basic submarine. Figures 19.4-19.9 also apply to the basic submarine except that the ℓ_T/GJ_e of the rudder stock has been increased to 2.8×10^{-4} (basic = 1.75×10^{-4}) ton^{-1} ft^{-1}; see Figure 2. Similarly, Figures 19.16-19.22 are for the basic submarine except that the rudders and stabilizers are attached to the hull one cell (10 ft) farther forward.

Critical Velocity versus Several Rudder Parameters for Basic Submarine

Figure 20 shows a plot of the critical velocity versus several rudder parameters (torsional flexibility ℓ_T/GJ_e, bending flexibility ℓ/EI, yaw inertia I_z, rudder mass M_y) for the basic hull.

The values of the electrical elements, discussed in Appendix A, have been calculated in Table 3.

ANALYTICAL RESULTS

An analytical method of solution for the flutter speed and frequency of a cantilevered control surface, devised in Appendix E, has been applied to the case of the cantilevered rudder system. Table 4 shows that the results of the calculation, using the same data as for the analog computation (Figure 2), are a flutter speed of 90 knots and a flutter frequency of 516 cpm.

DISCUSSION

MODES

The node lines of the cantilevered rudder shown in Figure 4 are linear because the rudder was treated as a rigid planar body.[6] The approximately horizontal node line for the first mode (relatively) indicates that this mode is predominately a bending mode. The second and third modes are more nearly torsion modes. Since both the first and second mode node lines nearly pass through the bending center of the rudder stock, very little change would occur in these modes if the motion were constrained to zero at this point. Therefore, these modes (the ones in which the rudder and submarine become unstable) are predominately rotations about the bending center. A similar statement for the center of mass is that mass changes (not moments of inertia) would strongly affect the first mode but not the second and third modes. Table 2.1 shows the close agreement between the analog results obtained here and the digital results obtained in Reference 6.

A comparison of the results in Tables 2.1 and 2.2 indicates that the frequency of the cantilevered stabilizer-diving plane system lies above the second frequency of the rudder. The first mode is predominately twisting of the diving plane, whereas the second mode is predominately bending of the stabilizer.

Table 2.3 shows the close approximation between the analog results for the hull modes (horizontal bending with no rudders) and the digital results obtained in Reference 6 for bending. A comparison of the torsion and bending modes for the hull only (see Table 2.4 and Figures 5.1-5.3) indicates that the first torsion mode frequency lies between the second and third bending mode frequencies.

A comparison of the frequencies for the hull only and for the hull with rigid appendages (see Table 2.4) shows that for the latter case the corresponding frequencies have all been reduced. This is due to the added mass. Figures 5.1-5.5 and 5.7 show that relatively minor changes occur in the mode shapes for bending but that substantial changes occur in the mode shape for torsion. The center of mass of the rudders is at approximately Hull Station 1.35 so that the y of the rudders should agree with the y of the hull at that station.

A study of Table 2.4 and Figures 5.9-5.15 reveals that the first bending mode (Figure 5.9) is essentially the same as that with rigid rudders (Figure 5.4) except that the frequency is lower due to more flexibility. The rudders move in the same direction as the hull. The second bending mode (Figure 5.10) is almost entirely the rudder mode (see Table 2.1 and Figure 4) with the maximum hull motion about 10 percent of the rudder center of mass. The frequency is slightly above that of the cantilevered rudder.

The third and fourth bending modes (Figures 5.11 and 5.12, respectively) are essentially the second and third hull bending modes (see Table 2.4 and Figure 5.5). The first torsion mode shown in Figure 5.13 has a sharp break in the curve at Station 1.5 due to the lack of inertia at Station 0.5. (See Table 1 in which the inertia at Station 0.5 was taken at zero because the inertia here is quite negligible. This explains the mode shapes of the torsion modes which show the same value at Station 0.5 as at Station 1.5.) The torque is therefore transmitted into the empennage at Station 1.5. This mode is predominately one of rudder bending; upper positive and lower negative. The second torsion mode is predominately hull torsion, and the third torsion mode is predominately diving plane motion.

Hull mode frequencies including mass coupling are (see Table 2.5) primarily (1) first hull bending, (2) second hull bending, and (3) first hull torsion frequencies.

FLUTTER

It is of interest to consider whether the rudders of the submarine will be subject to flutter at speeds within or near the operating range of the ship. The designer would also like to know if there is a loss of damping at velocities less than critical velocity. This could result in excessive vibrations. Significant also to the designer and analyst is the question of the role of the hull in flutter analysis. How much difference is there between the response of the cantilevered rudder and the response of the rudder mounted on a flexible hull? We will attempt to answer these questions for ALBACORE.

Figure 6 (basic curve, L = 0.3 ft) shows that as the velocity is increased from zero knots, the damping increases until S = 70 knots, then decreases to zero at 87 knots, and

then becomes unstable. Moreover, damping does not decrease below the damping at $S = 0$ until almost the critical velocity. The damping values for the cantilevered rudder and for the rudder attached to the hull differ only slightly, and the critical velocities for these cases are indistinguishable.

Nothing of interest occurred in the range of zero to 50 knots. The value L required to make the critical velocity fall in this range is unrealistic (see Figure 6 in which the effect of the center of pressure, arbitrarily moved forward, on the critical velocity is shown; see Figure 2 also). Figure 13 of Reference 5 shows that $L < 0.35$ ft; as explained previously, the sign convention in that figure is opposite to that used here. We infer from these observations that the basic system *with damping* will also be stable.

Figure 7 indicates that the three modes of the cantilevered rudder are lightly damped at $S = 0$. As the velocity is increased, the damping of all roots increases (for a finite range of velocities), and eventually the lower two frequencies (354 and 730 cpm) begin to approach each other. For $S/S_o > 1.2$, only two modes are *observable*. This behavior of two frequencies approaching each other and then going unstable is called frequency coalescence.[13] The third root continues to become increasingly stable and plays almost no part in the flutter.

Figure 8 indicates the same behavior in terms of amplitude γ versus frequency. Figures 8.1-8.5 show that as the velocity increases the peaks become rounder (due to greater damping) and approach each other (frequency coalescence). Figures 8.6-8.10, for the hull included, present similar features except that many additional peaks (modes) are introduced. The primary effect of the hull is to act as a vibration

damper at some frequencies and decrease the amplitude γ. The major peaks are virtually the same as before. At $S/S_o = 0$, the modes of the rudder can be seen at a little under 390 cpm and at about 770 cpm. These two modes approach each other with increasing S/S_o and then go unstable. Only when $S/S_o > 1.6$ does the amplitude of the unstable mode surpass that of the first bending mode. A comparison of Figures 8.11-8.15 and 8.16-8.21a shows that for the hull the major effect of damping is to decrease its response and shift its frequencies somewhat. A comparison of Figures 8.22-8.26 (rudder with damping) and 8.6-8.10 (no damping) shows that for the rudder the chief effect of damping is to increase the critical velocity.

In sum, Figure 8 illustrates the following interesting characteristics:

1. The behavior of the rudder is about the same whether it is cantilevered or attached to the flexible hull.

2. The major effect of the rudder-hull interaction is that the hull acts as a vibration damper at certain frequencies.

3. No large change in the character of the solution occurs when damping is introduced.

4. Even with damping present, the instability followed frequency coalescence of the rudder modes.

Figure 9 presents the response of the hull when the center of pressure was moved forward. At $S = 0$, the hull is less affected by the rudder mode. No solution was obtained at $S/S_o = 1.4$ because the system had a divergence (amplitudes increased without bound in an exponential rather than an oscillatory manner). Figure 10 shows

that no instability occurs for $S/S_o < 2.0$ when the center of pressure is moved aft of the rudder stock.

At $S/S_o = 0$, Figures 11.1-11.3 show that for the cantilevered stabilizer-diving plane system there is a distinct mode of the diving plane β and a poorly damped bending mode. For $0 < S/S_o < 2.0$, Figure 11.4 is indicative of the response of this system; i.e., the damping just continues to increase. The system is stable.

The effects of bending and torsion of the basic submarine, due to forcing of the lower rudder, upon the instability of the system is evident in Figure 12. The critical velocity occurs slightly above $S/S_o = 1.8$, which is about the same as for the rudder-hull system or cantilevered rudder. A study of Figures 12.1, 12.5, 12.9, and 12.13 reveals that as the flutter condition is approached the two lowest mode frequencies tend towards coalescence. The y-motion of the rudder is affected by the first hull mode at $S = 0$, but the rudder modes always dominate the response. The primary response of the hull is due to the hull modes until just before instability occurs. The major effect of the rudder on the hull is to increase (act as an amplifier) the force transmitted by the rudder into the hull at the resonant frequencies of the rudder.

Figure 13 shows the effect on the basic submarine when the rudder and diving plane flexibilities are increased by a factor of 4, thus lowering the critical velocity into the range of interest (<50 knots). It is known that for the cantilevered rudder this will reduce the critical velocity by a factor of 2 (as is evidenced by Figures 13.5-13.6). The order of the modes has changed so that the rudder mode is lowest and is followed by the hull bending mode. Flutter occurs at $S/S_o \approx 0.9$ [about one-

half the value with basic flexibility and at a frequency of 270 cpm (one-half the basic flutter frequency; see Figure 7 or 12.13)]. Thus the effect of the change in appendage flexibility upon the cantilevered rudder and upon the rudder of the basic submarine is the same. Figures 13.1-13.4 show the effects on the hull motion also.

Figure 14 presents the effect of mass coupling between lateral motion and roll of the hull on the response of the system.* (See $\bar{z}$ in Table 1.) This effect might be due partially to the effect of the sail. A comparison of Figures 12 and 14 indicates no substantial difference in the results due to the inclusion of mass coupling (note that Figure 14.17 was apparently clipped at the bottom). Figure 14.7 typifies the response of the upper rudder. Since the force was applied to the lower rudder, the hydrodynamic forces on the upper rudder inhibit motion until the critical velocity is reached, at which time the upper rudder goes suddenly unstable. At subcritical velocities, the motion of the upper rudder is small.

Figure 15 shows the effect of h (location of the rudder center of gravity aft of the rudder stock) on flutter of the cantilevered rudder. Figure 15.1 indicates that a steep crossing of the curve of damping g versus S/S_o occurs for the basic case. This signifies that large positive values of damping exist for velocities less than the critical value. As the center of gravity moves farther aft ($h > h_{basic}$), keeping the moment of inertia about the center of gravity constant, the critical velocity decreases. Moving the center of gravity forward ($h < h_{basic}$) increases the critical speed but decreases

*In terms of critical velocity, the value would be the same if $\bar{z}$ were taken to be negative, since the submarine is symmetric about the x-y plane in all other respects.

the steepness of the crossing. Finally a point is reached at which flutter no longer occurs ($h \approx -0.25$ ft). If the center of pressure lies aft of the center of mass, flutter does not occur. For this case (in the velocity range of interest), a loss of damping (subcritical flutter) takes place without any instability. Figure 15.2 shows that adding mass to change flutter speed is relatively ineffective. The mass is predominately virtual mass which cannot be shifted.

Figure 16 indicates that the effect of shifting the cantilevered rudder mass and center of pressure, (i.e., h and L)* with respect to the rudder stock, on the critical velocity or steepness of the damping curve is small. Moving the rudder forward ($h = 0.986$, $L = 0.80$) tends to decrease the critical velocity. Flutter can still occur even though the center of pressure is aft of the rudder stock. (e.g., $h = 1.986$ and $L = -0.2$).

Examination of the numbers in Figure 17 shows that the motion of the upper rudder is about 1 percent or less of the corresponding motion on the lower rudder (which was forced) until just before flutter occurs. The diving plane and stabilizer also have quite small motions. The forces in the rudder stock and hull decrease from their values at zero velocity and then grow rapidly as flutter approaches. At zero velocity the hull seems to be in a third bending mode and first torsion mode (4 and 1 node lines, respectively). As the velocity increases, the phase makes it difficult to identify the mode. The largest hull motion at intermediate velocities is at the bow. At a velocity

*h and L are taken positive aft and forward of the rudder stock, respectively (see Figure 2).

of $S/S_o = 1.8$, the hull is in a second bending mode and first torsion mode, and the amplitude at the stern is largest. Except for velocities near the critical value, hull motion is small compared to rudder motion.

In aeroelastic flutter, one parameter frequently studied is the aerodynamic pitch damping proportional to the velocity. This term, for the cantilevered rudder, is similar to c, except for the velocity dependence. Thus if $C_{\dot{\gamma}}$ is the pitch damping per unit velocity, then $c = C_{\dot{\gamma}} S$ is the pitch damping and $C_{\dot{\gamma}} S \dot{\gamma}$ is the damping moment. At $S/S_o = 1.85$ and $C_{\dot{\gamma}} = 0.01025$, $c = 1.6$, which is the basic value. Except for $C_{\dot{\gamma}} = 0$, the values of $C_{\dot{\gamma}}$ shown in Figure 18 yield values of c much larger than the basic value. Figure 18 shows this term to be stabilizing; i.e., its omission makes for a conservative estimate.

Figure 19 shows the magnitude of the lateral force applied to the basic submarine hull by the rudders at several frequencies. The figure also indicates the effect on the basic submarine of varying the torsional flexibility of the rudder stock and the position of the rudder and stabilizers. The force on the hull starts at about 1 ton for $S = 0$ and $\omega = 0$ and then varies with ω; at some frequencies, it is magnified to several tons due to resonance, as shown in Figure 19.3. Figures 19.12 and 19.15 show that the magnification is smaller at higher velocities. Figures 19.4-19.9 indicate that the effect of increasing the ℓ_T/GJ_e of the rudder stock by the indicated amount is to reduce the critical velocity to about $1.4\ S_o$. This shift in speed is related to the fact that the torsion frequency is brought nearer the bending frequency of the rudder so that coalescence occurs sooner (compare Figures 19.1 and 19.4; the highest peak is the

torsion mode). Figures 9.16-9.22 show the effects of attaching the rudder and stabilizer to the hull one cell forward; the character of the solutions is very similar to the basic case (Figures 9.10-9.15).

Figure 20 shows the effect of four of the rudder parameters on the basic submarine. If the torsion of the rudder stock is made more flexible (increasing ℓ_T/GJ_e) or its bending more rigid (decreasing ℓ/EI), it is expected that the critical velocity will decrease as is shown (i.e., frequency coalescence will occur earlier). Increasing the yaw moment of inertia also lowers the torsion frequency and hence the critical velocity. Decreasing the rudder mass from its basic value will raise the bending frequency, and Figure 20 shows that this will lower the critical speed. For the range of parameters studied, both the bending flexibility and the mass showed minimums which give the lowest critical velocity.

Comparison of Table 4 and Figures 6 and 7 shows that the analytical and electric analog solutions for the flutter speed and frequency of ALBACORE are in excellent agreement; that is, approximately 3 percent and 1 percent, respectively. Since the hull of ALBACORE has little effect upon the motions of the rudder, the analytical method of solution *for this cantilevered rudder* is as suitable as the analog method for predicting instability whether actually cantilevered or attached to the hull.*

CONCLUSIONS

For ALBACORE the following conclusions are presented with regard to the nature of the flutter, the interaction of the appendage parameters, and the modes.

*However, other studies indicate that this result for ALBACORE may not be true in general (see, for example, Reference 19). The point remains to be resolved by further investigation

1. For the basic configuration of ALBACORE shown in Figure 2, the motion of the rudders will become increasingly stable (i.e., rudder damping will increase rapidly) with velocity until a velocity is reached that is slightly less than the critical value (90 knots), where the rudder becomes unstable. Due to the sudden onset of flutter versus velocity, subcritical flutter (small system damping without instability) is *not* a problem. Flutter here is a classical frequency coalescence between the bending and torsion modes of the rudder, and parameter changes which bring these two modes together will, in general, lower the velocity.

2. The hull has little effect upon the motions of the rudder. The very large mass and roll inertia of the hull effectively cantilever the rudder at subcritical velocities so that results for a cantilevered rudder closely approximate those for the rudders attached to the hull. *Hence, the analytical method of solution for the cantilevered rudder of* ALBACORE *(see Appendix E and Table 4) is as suitable as the analog method for predicting its instability (flutter speed and frequency) whether actually cantilevered or attached to the hull.** Interaction has two effects: (1) the response of the rudder to sinusoidal forces is decreased at frequencies near the free modes of the hull and (2) the response of the hull is increased at the cantilevered frequencies of the rudder. Matching the hull frequency to the flutter frequency will not assist in preventing flutter through the absorption effect of the hull (the attempt to do so failed). Modification of appendage flexibilities by a factor of 4 to make the rudder frequency lower than the hull frequency does not change the nature of the interaction.

*However, extension of this conclusion for ALBACORE to control surfaces in general is clearly unwarranted at this time. As stated in the footnote on Page 23 the subject requires further investigation.

3. Increasing the rudder torsional flexibility, decreasing the rudder bending flexibility, increasing the rudder yaw moment of inertia, and decreasing the rudder mass, all of which tend to make the bending and torsion mode frequencies closer together, decrease the critical velocity. Increasing appendage flexibilities by a factor of 4 decreases the critical velocity by a factor of 2. Moving the center of pressure forward decreases the flutter speed. Damping terms, associated with the yaw and lateral motion of the rudder, whose values lie between no damping and the basic values (Figure 2), have little effect upon the results. Increasing yaw damping to larger values stabilizes the system. Moving the complete rudder mass and center of pressure has little effect on the critical velocity or steepness of the damping versus velocity curve. Moving the rudder forward tends to slightly decrease the critical speed, i.e., is slightly destabilizing. Flutter does not occur when the center of pressure is aft of the center of mass.

4. The diving plane does not flutter (undoubtedly because the center of pressure of the diving plane was calculated to lie on the axis of rotation). The high rigidity of the stabilizer, which makes its mode frequency large compared with the rudder bending frequency, will prevent frequency coalescence in the velocity range of interest.

5. The natural frequencies of the uncoupled rudder and hull may be considered as rough approximations to some of the natural frequencies of the combined rudder hull system.*

*This was hypothesized in Reference 6 and found to be true in this study. It was observed that the hull bending mode frequencies decreased and the rudder mode frequencies increased when the two systems were joined. The converse should occur if the rudder frequencies were below the hull frequencies.[14, 15]

RECOMMENDATIONS

As ship speeds increase, severe vibrations or control-surface flutter may occur within the operating speed range.* It is therefore recommended that:

1. Computations similar to those presented here be made for high-speed ships (including hydrocraft) still in the design stage using the theories of References 8** and 5. The results can be used to design a ship (or its components) to prevent excessive vibrations or flutter.*** To permit the making of both electric analog and digital computations, the equations given in these references should be coded for the digital computer.

2. Analytical solutions for the flutter of a cantilevered control surface, similar to the solution obtained here for ALBACORE, should be determined for the control surfaces of high-speed ships. The results should be compared with the analog and/or digital results for an interacting control surface-hull system. This will permit a determination of the degree to which the analytical method can represent (and

*As evidenced by the severe vibrations transmitted to the hull of FORREST SHERMAN by the rudders during a steady horizontal turning maneuver[1,2] and by recent flutter model investigations.[3,4]

**The validity of the equations for the lift forces and moments given in Reference 8 is still to be determined. The theory, while having some degree of verification,[10] requires additional confirmation through further comparison with experiment. In particular, it is important to establish the conditions (range of parameters) for which it is valid. If corrections to the analytical description (equations) for the hydrodynamic forces and moments of Reference 8 are required, then only the hydrodynamic aspect of the equations and corresponding circuitry (of this reference) need be modified. Thus, the changes in the total circuitry and computer coding will be relatively slight.

***Such computations were performed recently on the PGM Motor Gunboat at the request of the Bureau of Ships.[16]

supersede) these computer methods for predicting the flutter instability of a control surface attached to a hull. In sum, it would be desirable, if design procedures are to be established, that simple computational methods with known reliability be developed.

3. Whenever possible, the computations should be verified by full-scale and/or model tests.[10]

ACKNOWLEDGMENTS

The authors gratefully acknowledge Messrs. G. F. Franz and E. F. Noonan for their constructive criticism of this report. Also, the authors wish to acknowledge Dr. W. J. Dixon of Computer Engineering Associates for his contribution to the present report.[16,17] Dr. E. H. Kennard collaborated with the authors in devising the analytic method of solution presented in Appendix E. Valuable suggestions made by Dr. E. Buchmann and Mr. Arthur Kilcullen during the course of this work are also gratefully acknowledged.

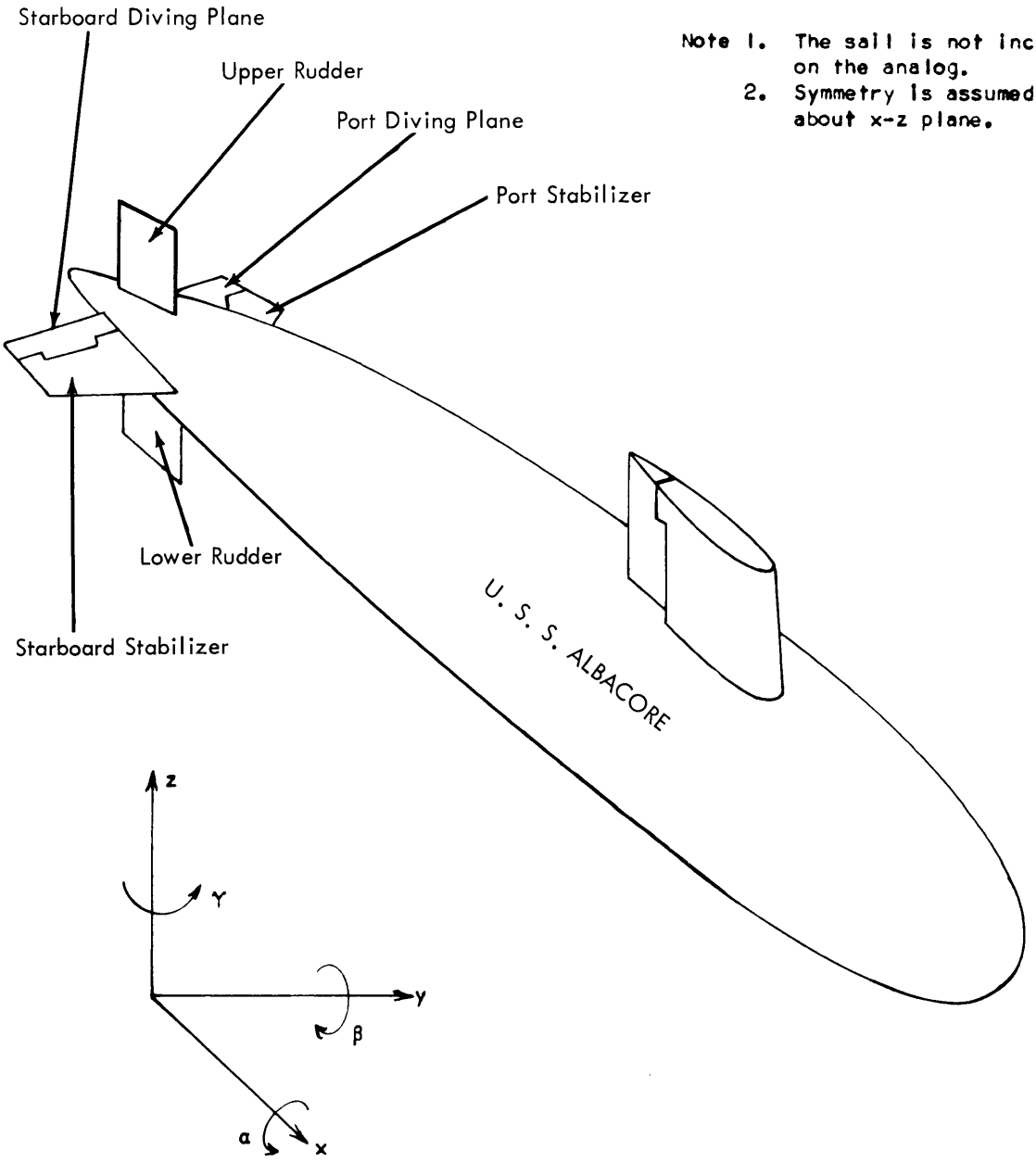

Figure 1 - Coordinate System of ALBACORE

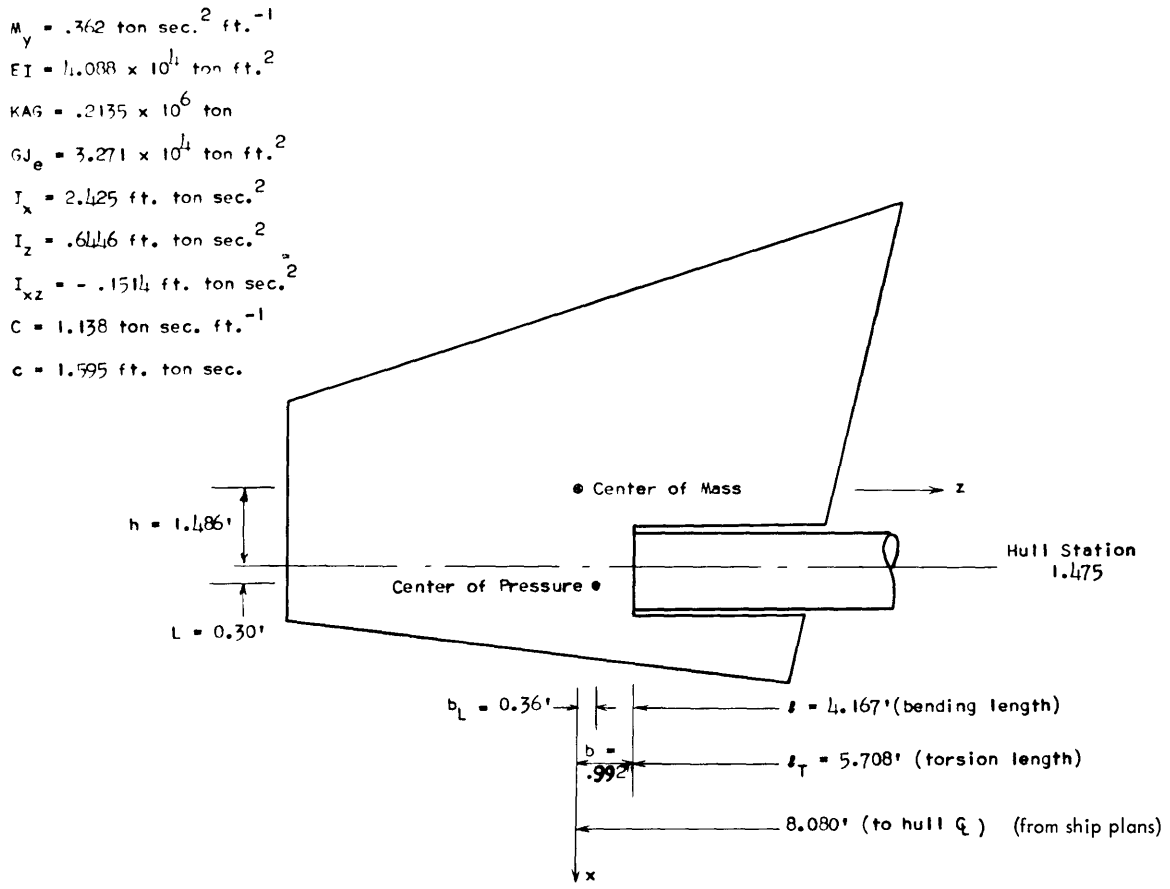

Figure 2 - View of Lower Rudder from Starboard (I.E., in Positive y-Direction) with Values of Rudder Parameters for the Basic Configuration

Note: These data are reproduced from Table 1 of Reference 5 with the exceptions of b_L and L. This reference lists two definitions for b_L in the list of symbols. The definition in this report agrees with the second definition, and the value given in Reference 5 is based upon the first definition which refers to a different dimension, and is therefore not used here. Here b_L = 0.36 ft (4.32 in.) was derived from a scaling of the figures of Reference 5 in which the rudder outline was superimposed on a drawing of the hull. In this drawing, the center of pressure was taken at 6.0 ft (72 in.) above the rudder tip. The value of L was taken from Figure 13 of Reference 5. A value of 0.30 ft forward of the rudder stock axis was used as an average value for a range of angles of attack up to 12 or 14 deg. (Table 2 of Reference 5 shows that the percent chord of the CP ranged from 19 percent at zero angle of attack to 27 percent at 30 deg angle. Therefore, in Figure 13 of that reference, negative values of L mean that the center of pressure is ahead of the rudder stock. In this report, the sign convention for L (see list of symbols) is opposite, hence L is positive in Figure 2.)

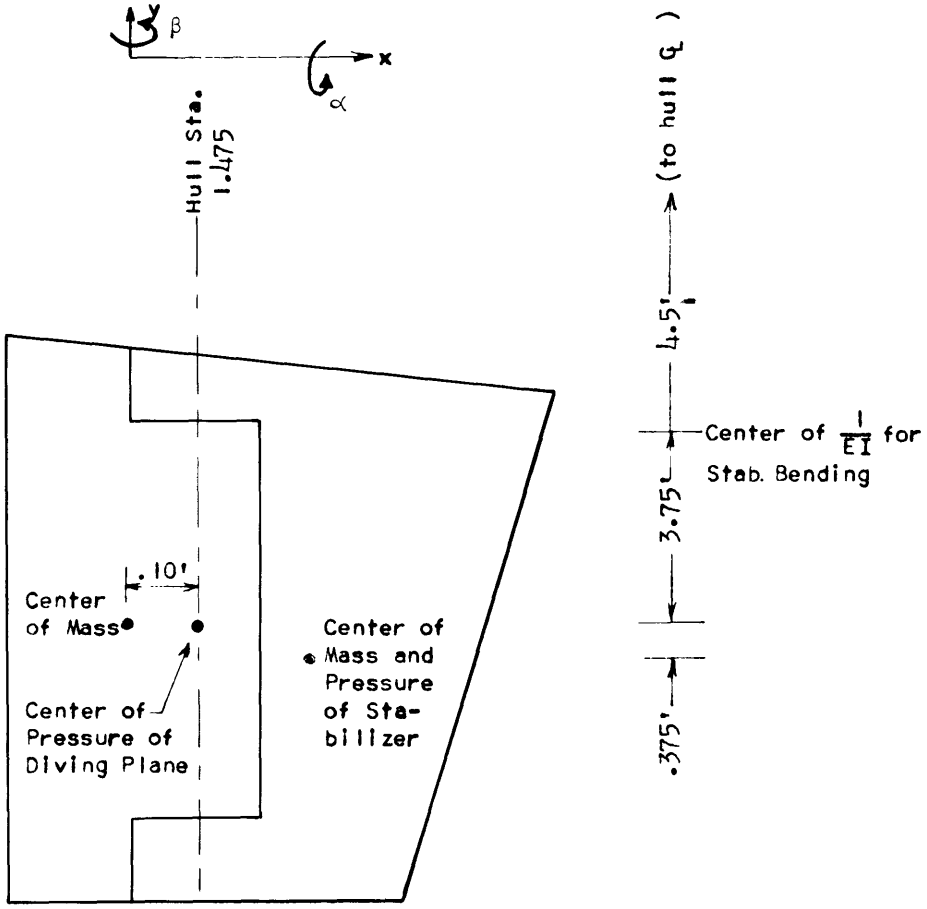

Not to scale

M_y = .212 ton sec.^{2} ft.$^{-1}$ (Stab. plus diving plane)

M_z = .844 ton sec.^{2} ft.$^{-1}$ (stab.)

M_z = .666 ton sec.^{2} ft.$^{-1}$ (diving plane)

I_{my} = .98 ton sec.^{2} ft. (diving plane)

I_{mz} = 18.88 ton sec.^{2} ft. (stab. plus diving plane)

Diving plane torsion spring 1.418×10^{-4} rad/ft.-ton

Stabilizer bending spring 1.85×10^{-6} rad/ft.-ton

The stabilizer has infinite torsion rigidity. This constraint makes it unnecessary to locate center of mass and center of pressure of stabilizer. I_{mx} of the stabilizer has been neglected. The diving plane has infinite bending rigidity. No zero velocity damping was added to stabilizer.

Figure 3 - Starboard Diving Plane and Stabilizer (Looking in the Negative z-Direction)

Note: Values of the parameters of this system were derived from ship plans.

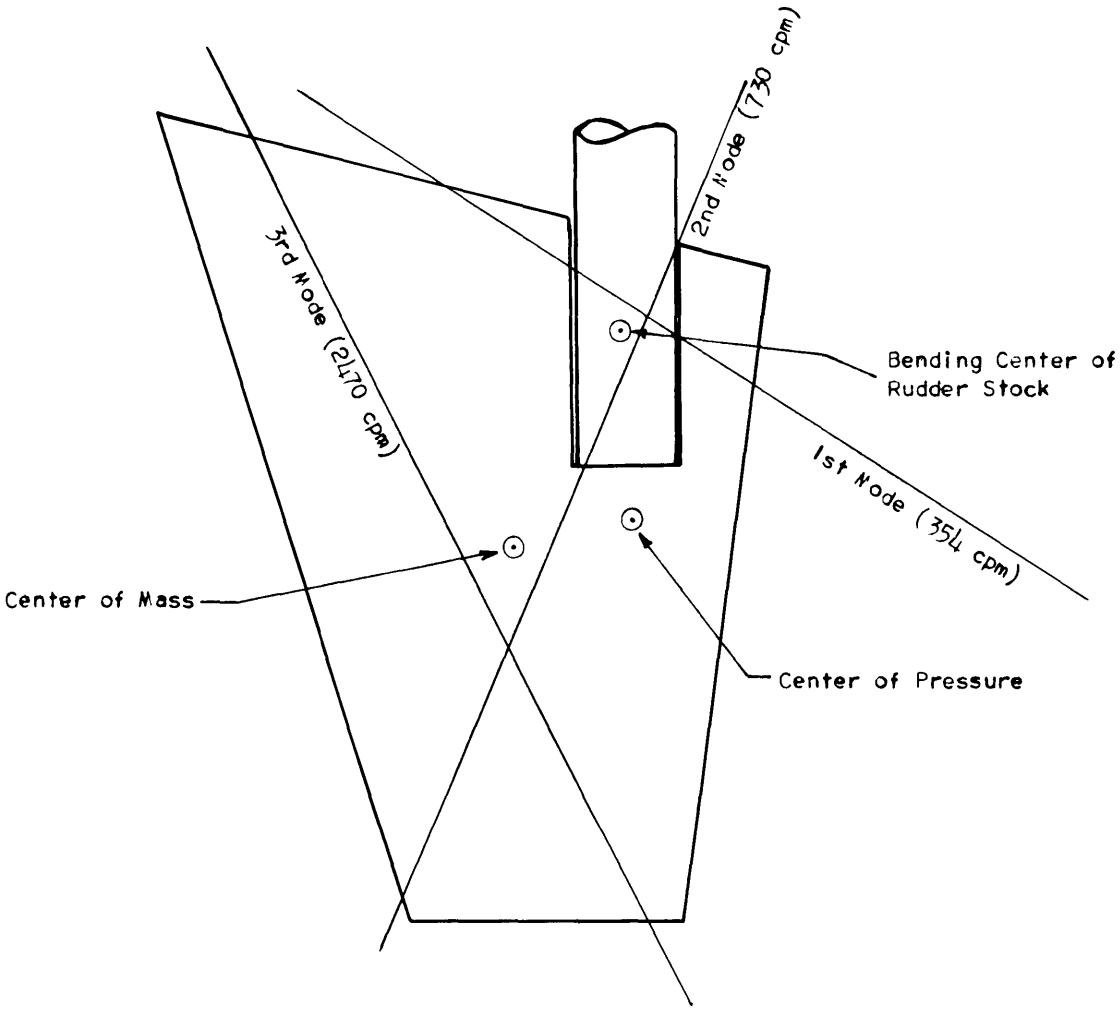

Figure 4 - Node Lines of Modes of Cantilevered Rudder
(Plotted to Scale)

Figure 5 - Hull Modes for ALBACORE

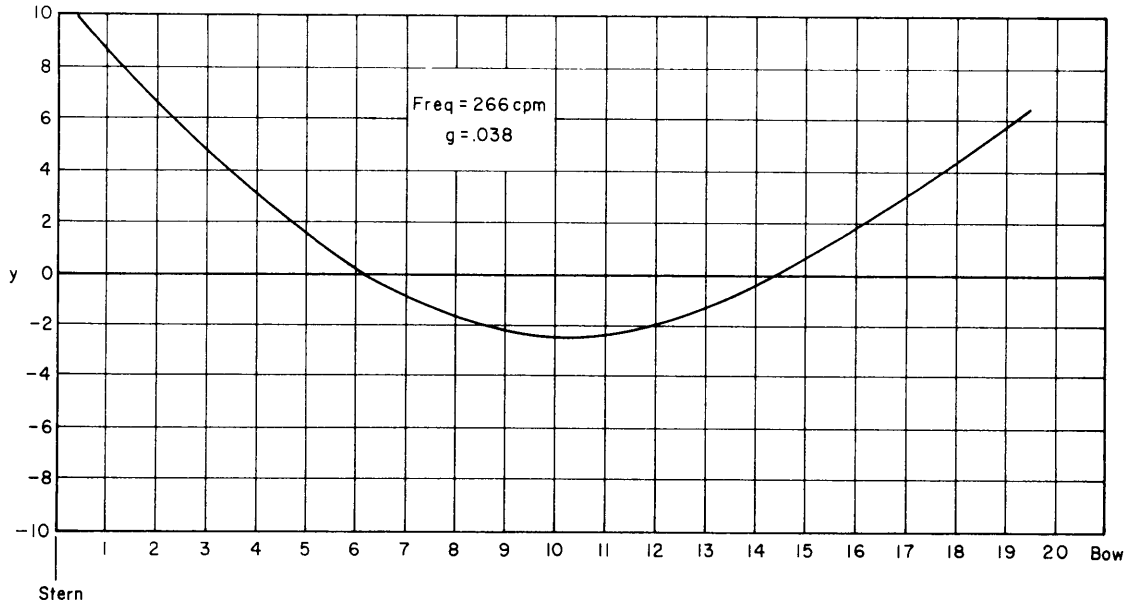

Figure 5.1 - Hull Bending Only - First Mode

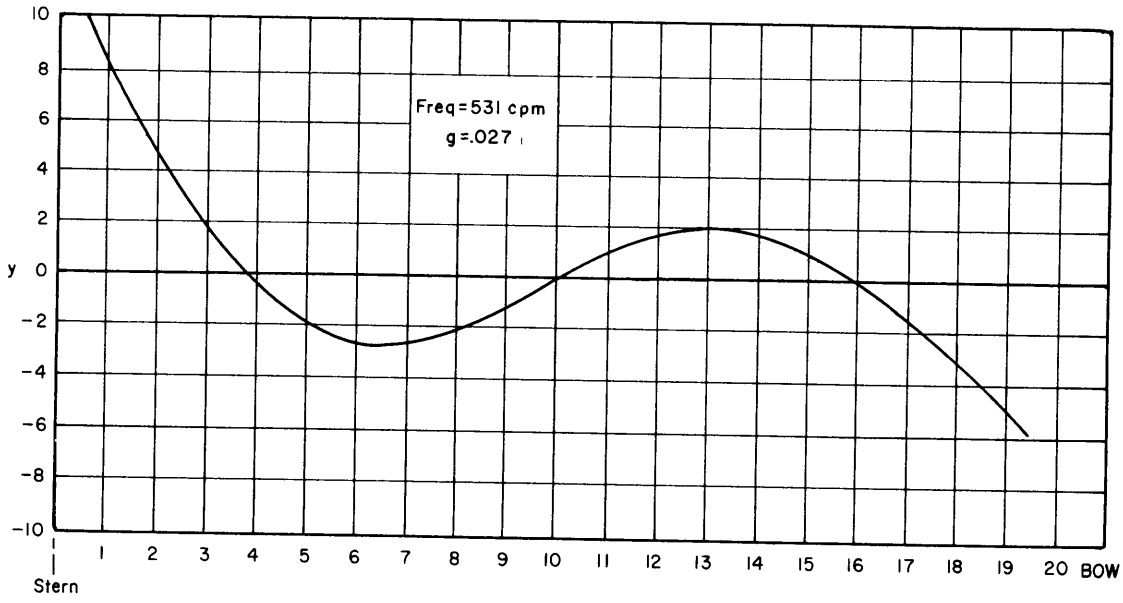

Figure 5.2 - Hull Bending Only - Second Mode

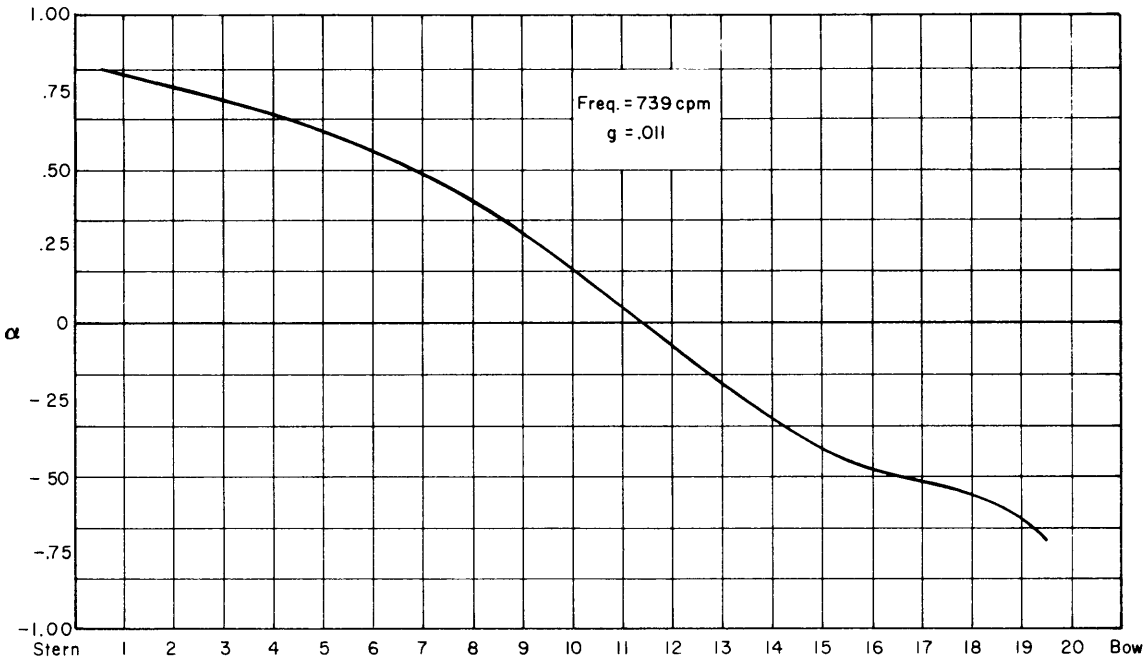

Figure 5.3 - Hull Torsion Only - First Mode

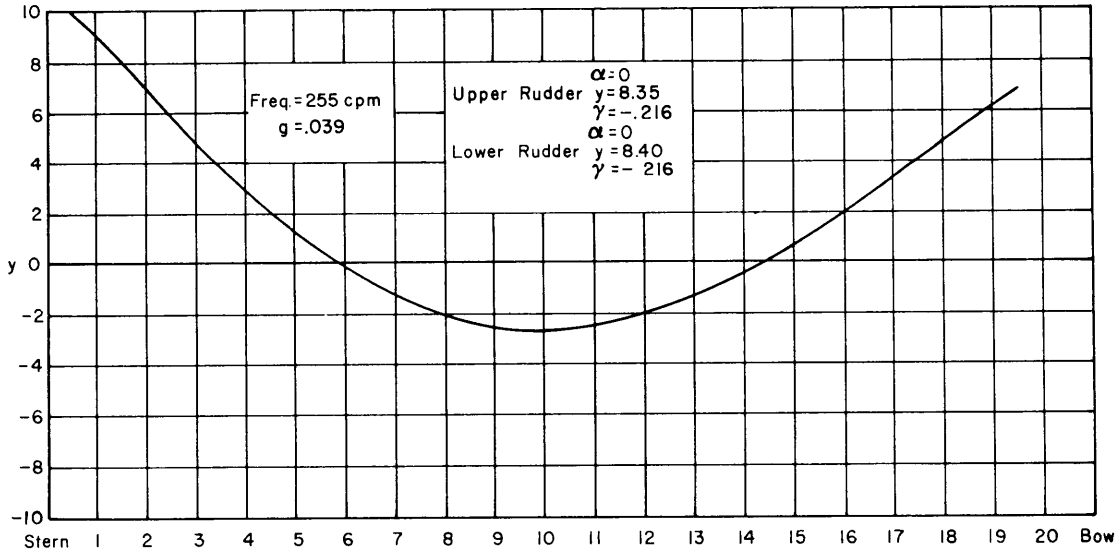

Figure 5.4 - Hull Bending with Rigid Rudders - First Mode

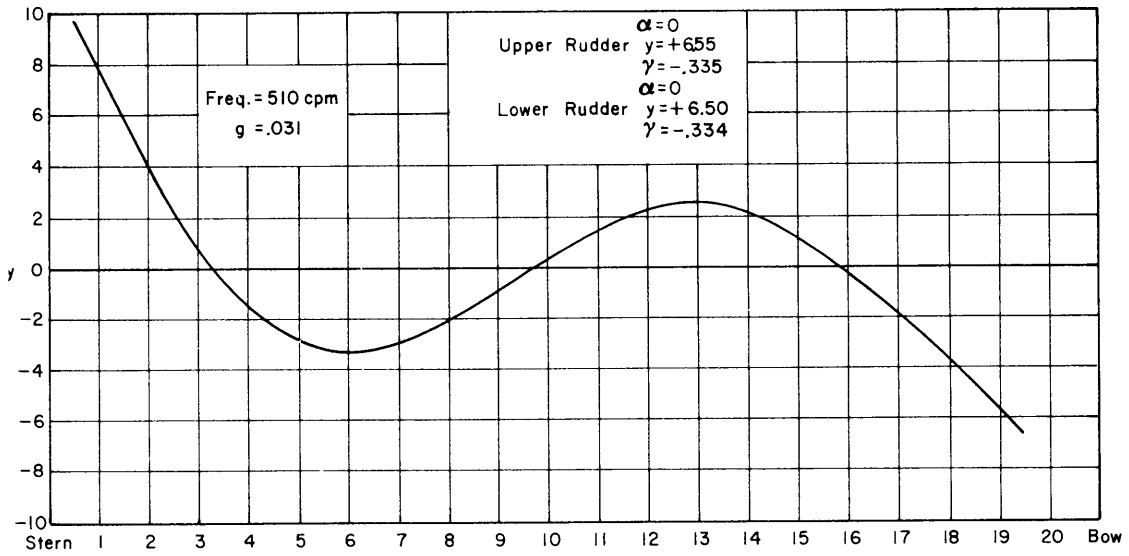

Figure 5.5 - Hull Bending with Rigid Rudders - Second Mode

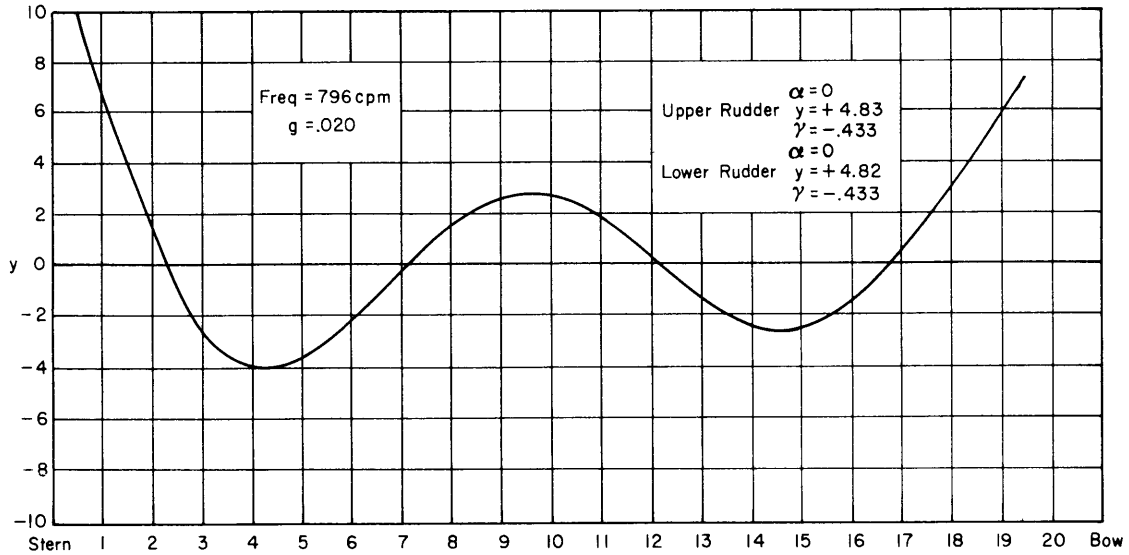

Figure 5.6 - Hull Bending with Rigid Rudders - Third Mode

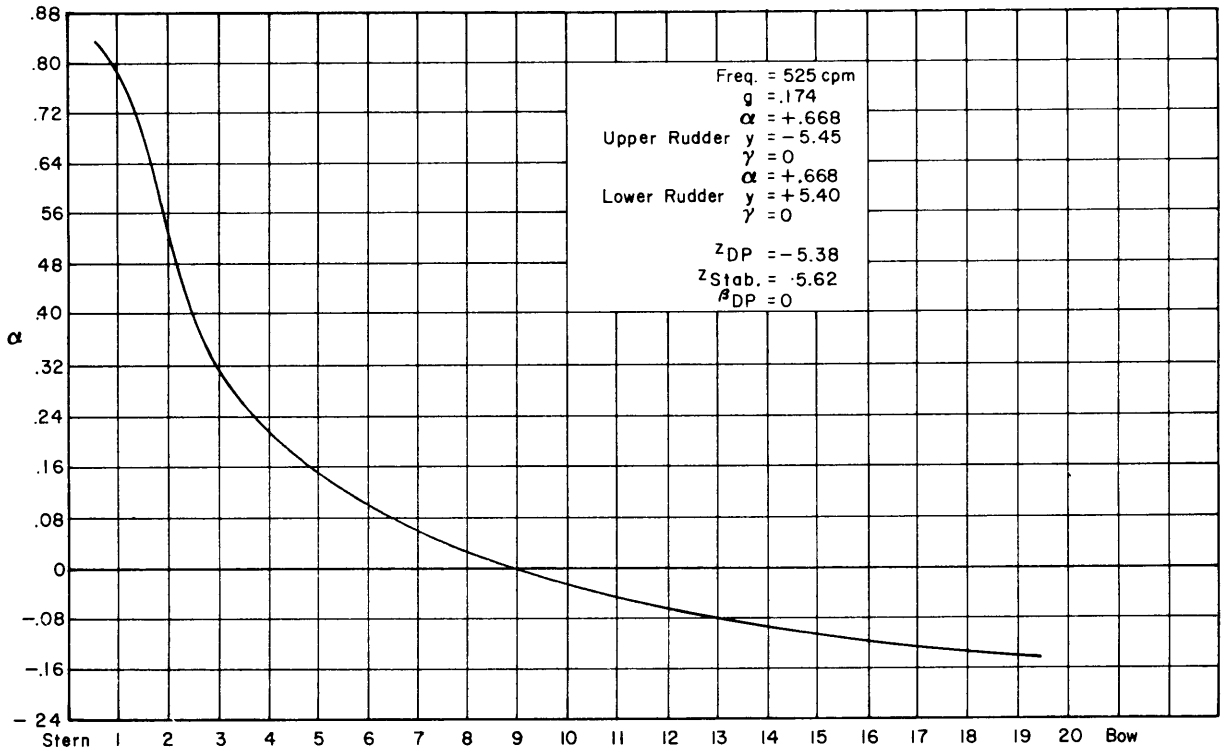

Figure 5.7 - Hull Torsion with Rigid Diving Planes and Rudders - First Mode

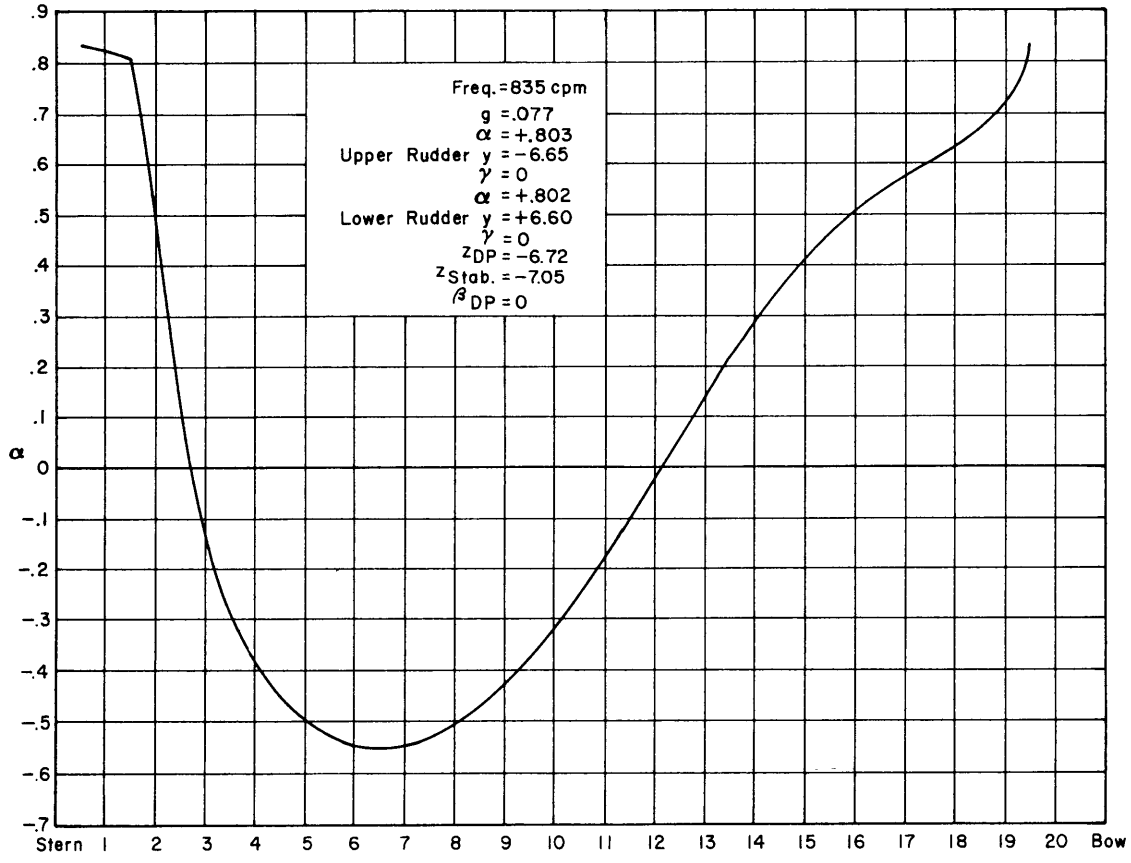

Figure 5.8 - Hull Torsion with Rigid Diving Planes and Rudders - Second Mode

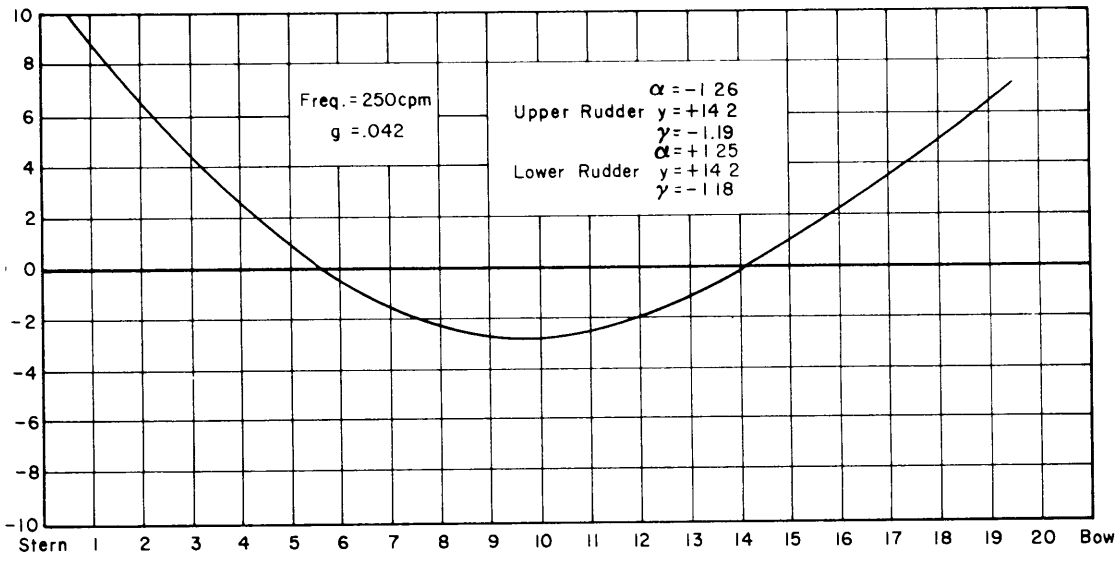

Figure 5.9 - Hull Bending with Flexible Rudders - First Mode

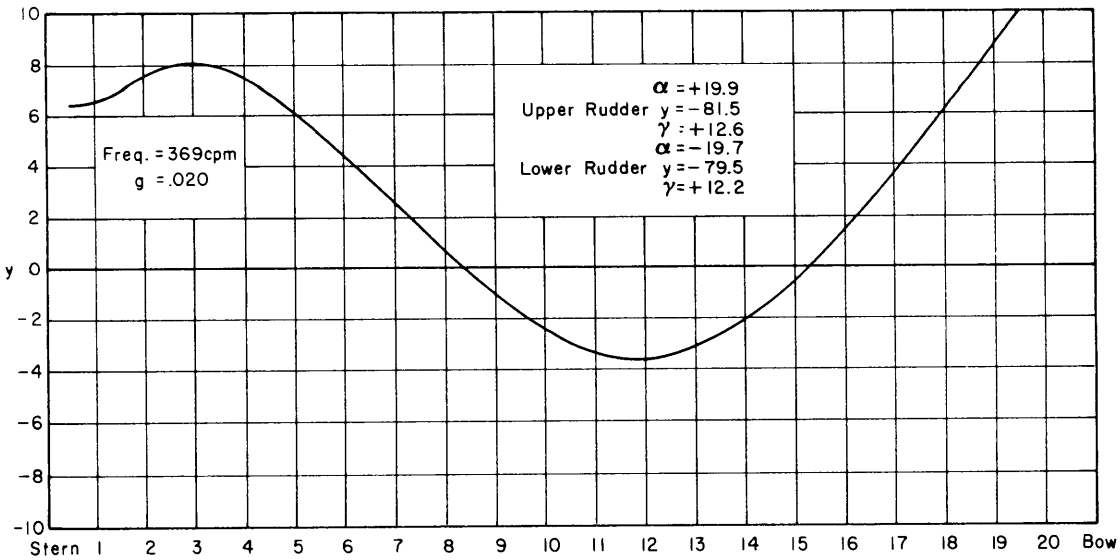

Figure 5.10 - Hull Bending with Flexible Rudders - Second Mode

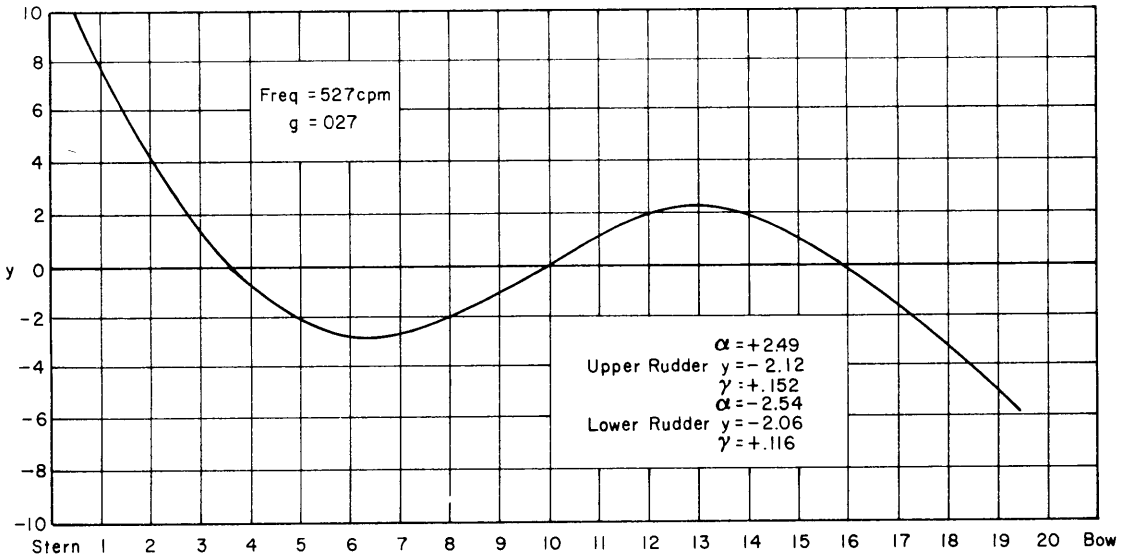

Figure 5.11 - Hull Bending with Flexible Rudders - Third Mode

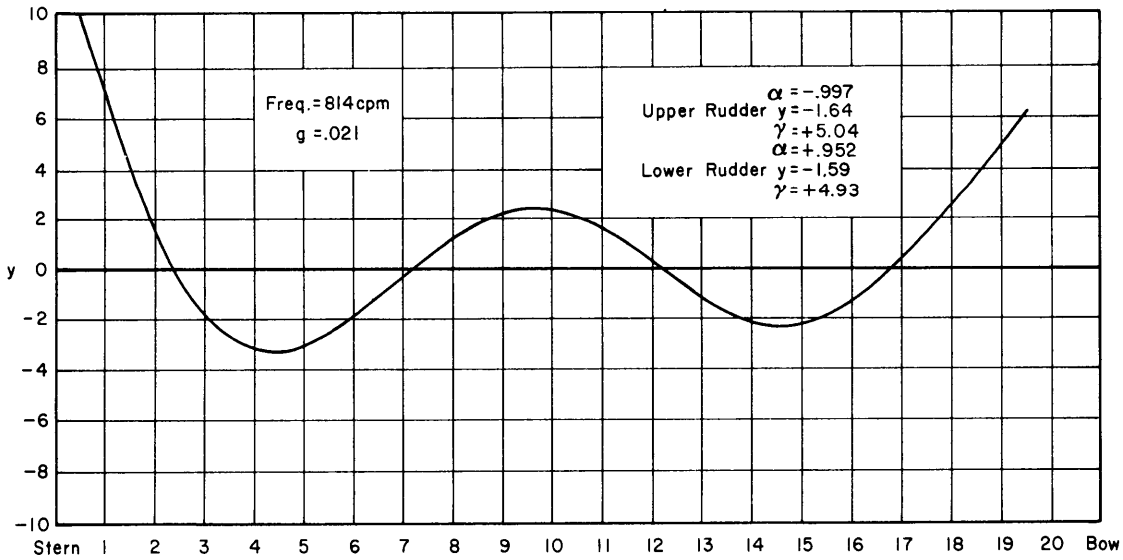

Figure 5.12 - Hull Bending with Flexible Rudders - Fourth Mode

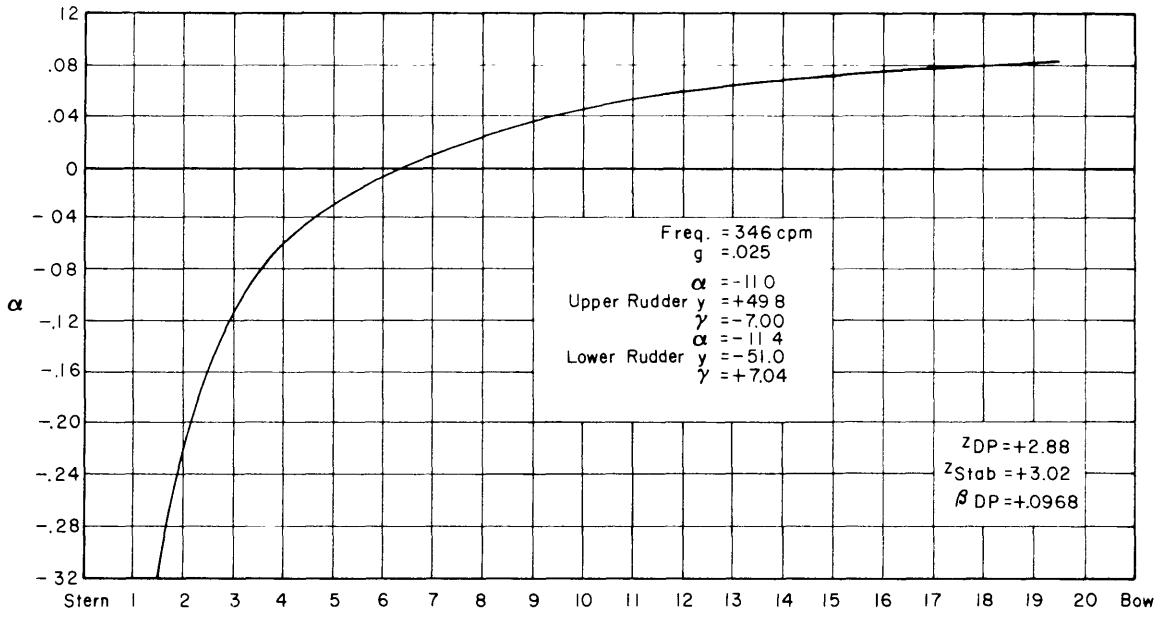

Figure 5.13 - Hull Torsion with Flexible Diving Planes and Rudders - First Mode

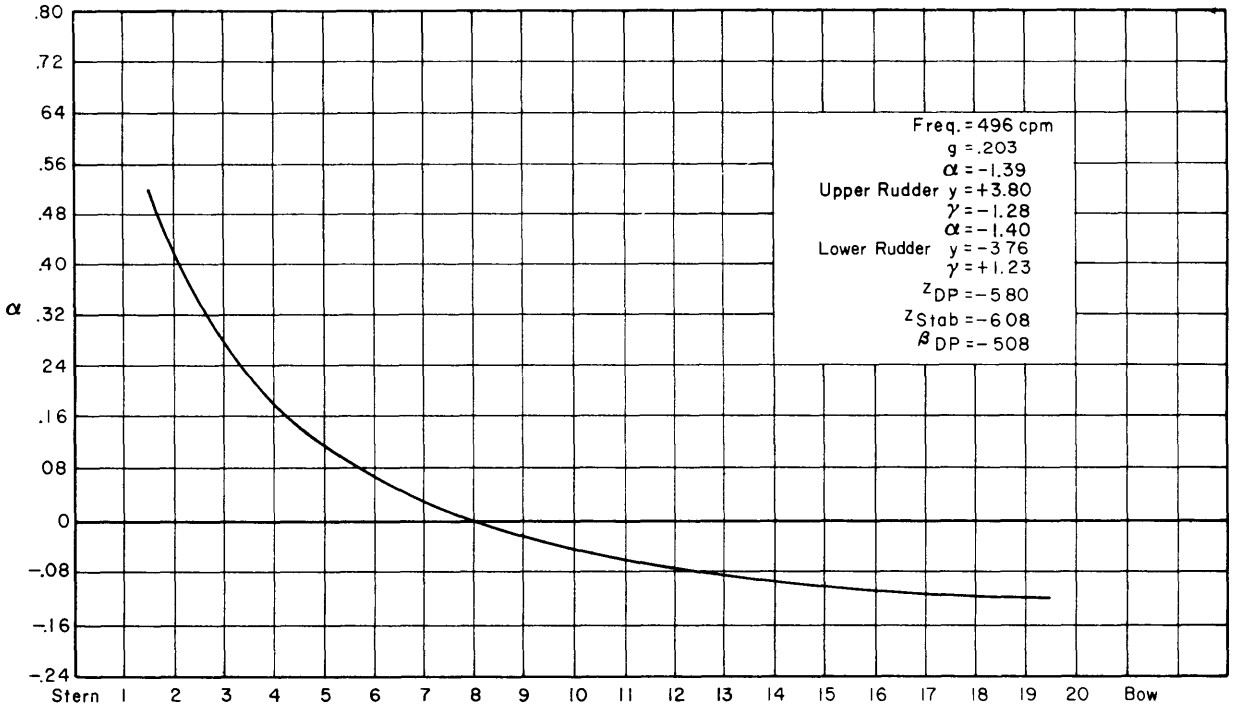

Figure 5.14 - Hull Torsion with Flexible Diving Planes and Rudders - Second Mode

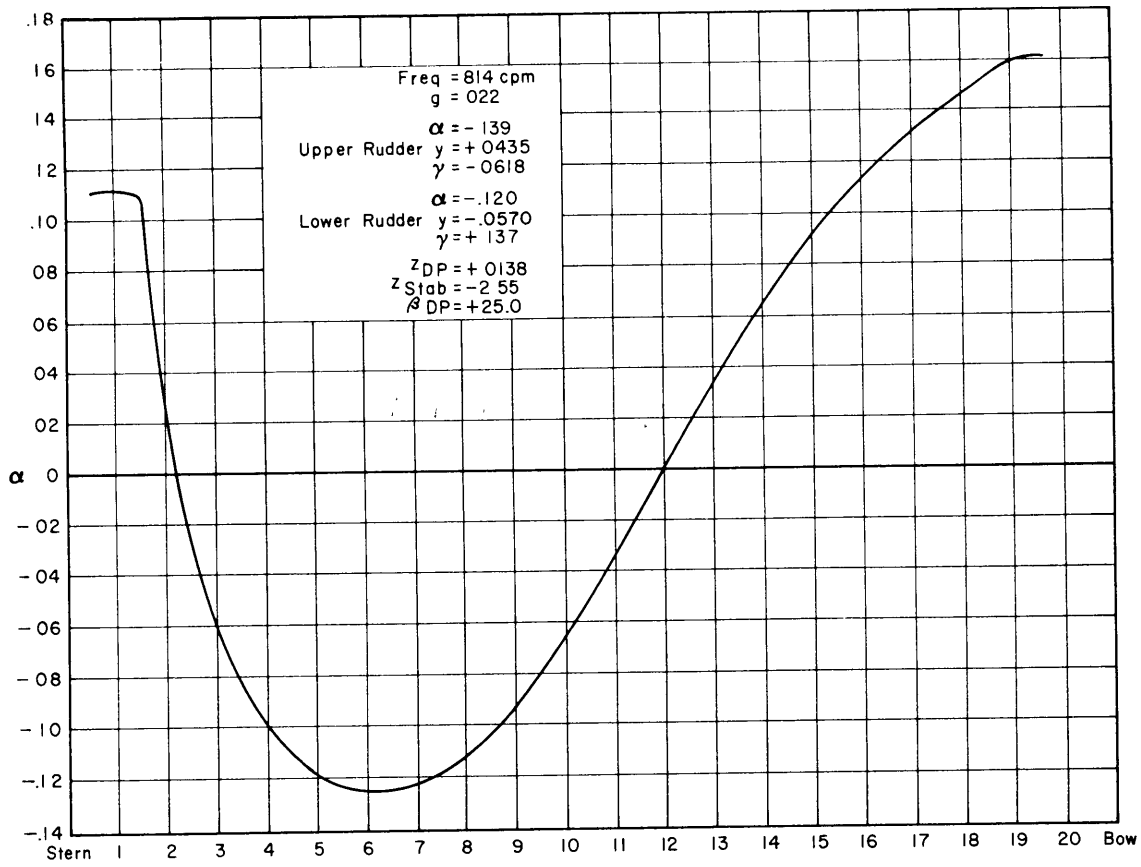

Figure 5.15 - Hull Torsion with Flexible Diving Planes and Rudders - Third Mode

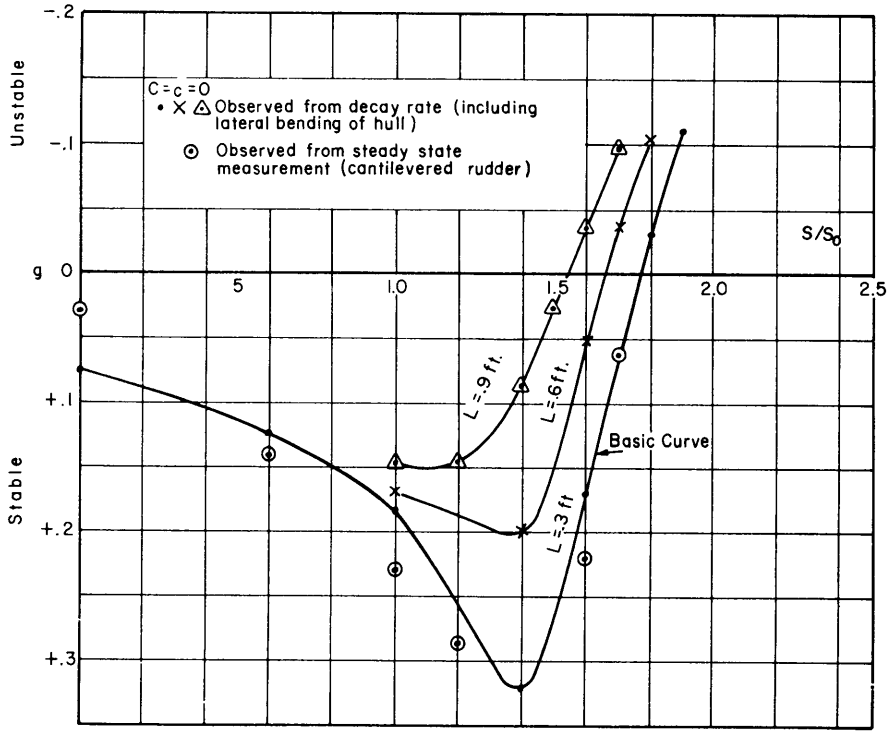

Figure 6 - Rudder Damping versus Velocity, C = c = 0; L Variable

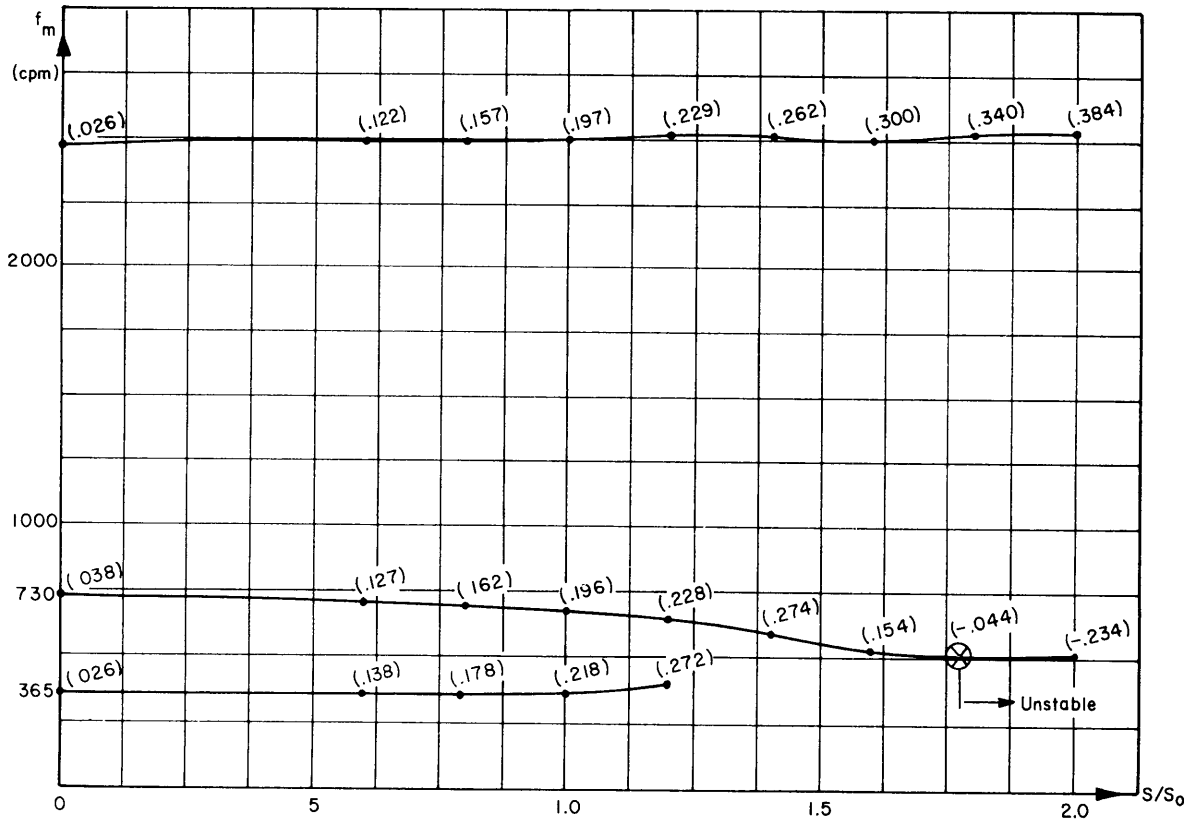

Figure 7 - Frequency and Damping of Cantilevered Rudder versus Velocity, C = c = 0. The numbers shown along the curve are the values of g.

Figure 8 - Amplitude Versus Frequency of (a) Cantilevered Rudder, (b) Rudder Attached to Hull, and (c) Hull; L = O

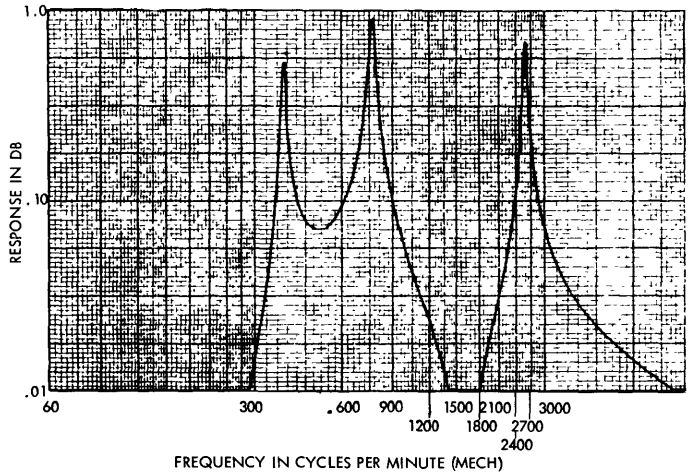

FREQUENCY IN CYCLES PER MINUTE (MECH)

Figure 8.1 System: Rudder with no damping
Force: Rudder Lift
Measure: Y-rudder
S/S_o=0

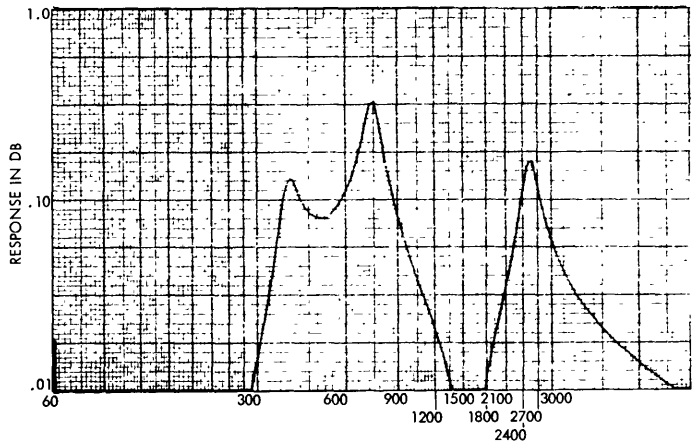

FREQUENCY IN CYCLES PER MINUTE (MECH)

Figure 8.2 System: Rudder with no damping
Force: Rudder Lift
Measure: Y-rudder
S/S_o=0.6

Note: Logarithmic scale on abscissae has been multiplied by 30. (See Appendix D)

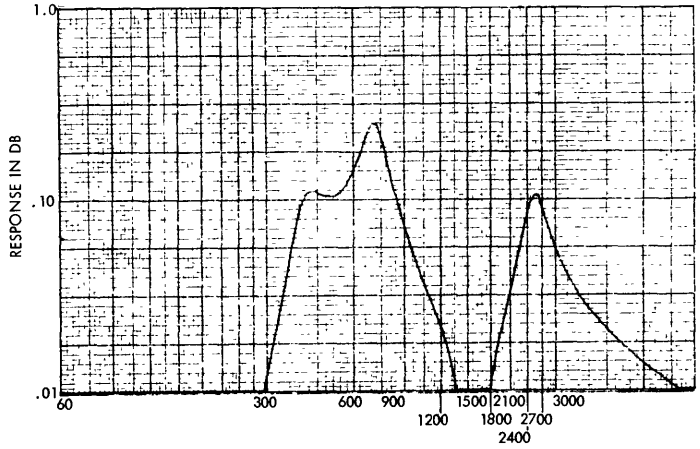

FREQUENCY IN CYCLES PER MINUTE (MECH)

Figure 8.3 System: Rudder with no damping
Force: Rudder Lift
Measure: Y-rudder
S/S_o=1.0

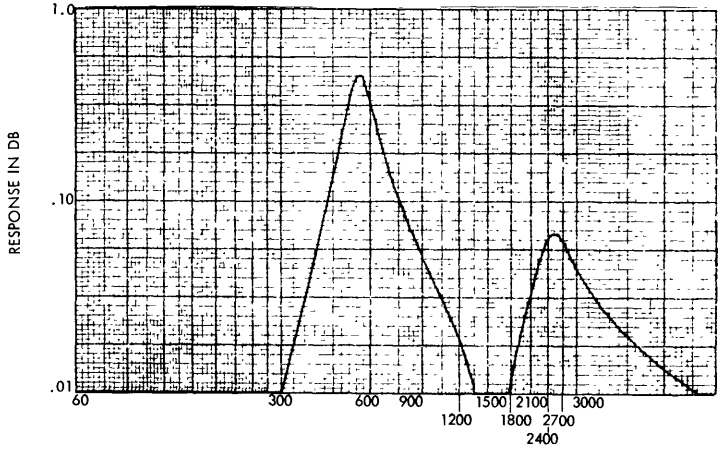

FREQUENCY IN CYCLES PER MINUTE (MECH)

Figure 8.4 System: Rudder with no damping
Force: Rudder Lift
Measure: Y-rudder
S/S_o=1.6

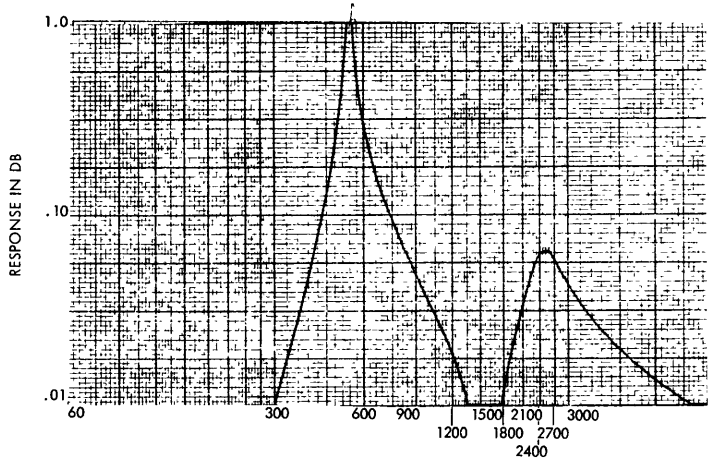

Figure 8.5 System: Rudder with no damping
Force: Rudder Lift
Measure: γ-rudder
S/S_o=1.7

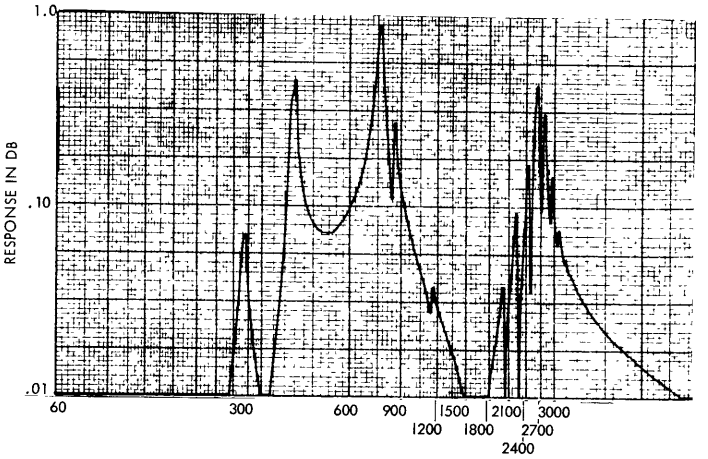

Figure 8.6 System: Rudders and Hull, no damping
Force: Symmetric Rudder Lift
Measure: γ-upper rudder
S/S_o=0

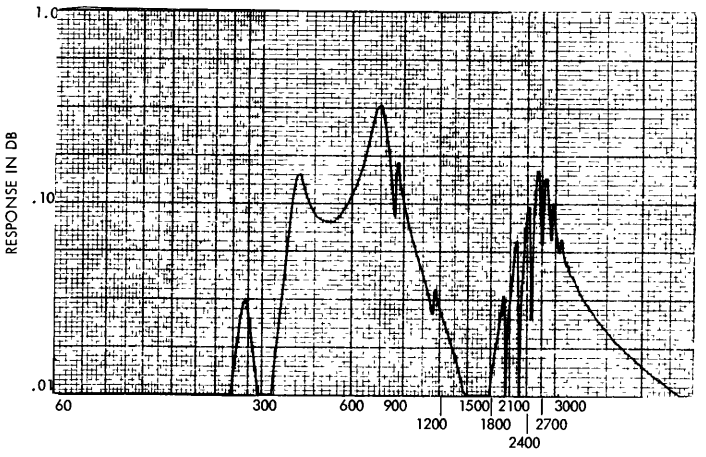

Figure 8.7 System: Rudders and Hull, no damping
Force: Symmetric Rudder Lift
Measure: γ-upper rudder
S/S_o=0.6

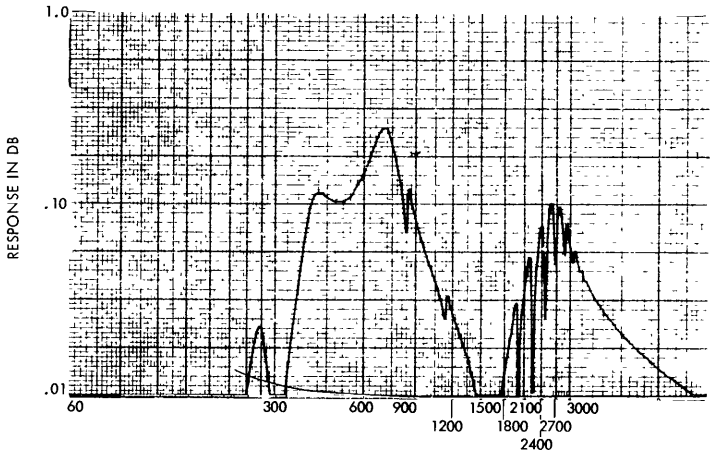

Figure 8.8 System: Rudders and Hull, no damping
Force: Symmetric Rudder Lift
Measure: γ-upper rudder
S/S_o=1.0

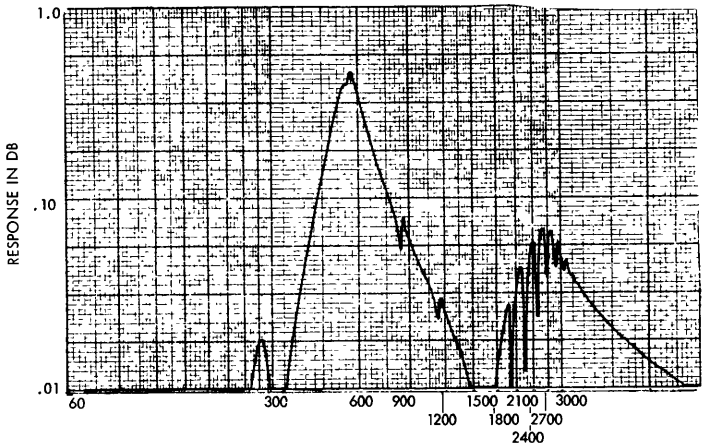

FREQUENCY IN CYCLES PER MINUTE (MECH)

Figure 8.9 System: Rudders and Hull, no damping
Force: Symmetric Rudder Lift
Measure: γ-upper rudder
S/S_o=1.6

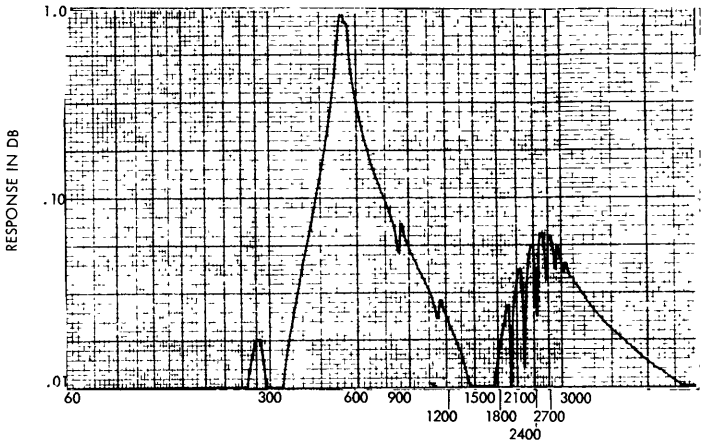

FREQUENCY IN CYCLES PER MINUTE (MECH)

Figure 8.10 System: Rudders and Hull, no damping
Force: Symmetric Rudder Lift
Measure: γ-upper rudder
S/S_o=1.7

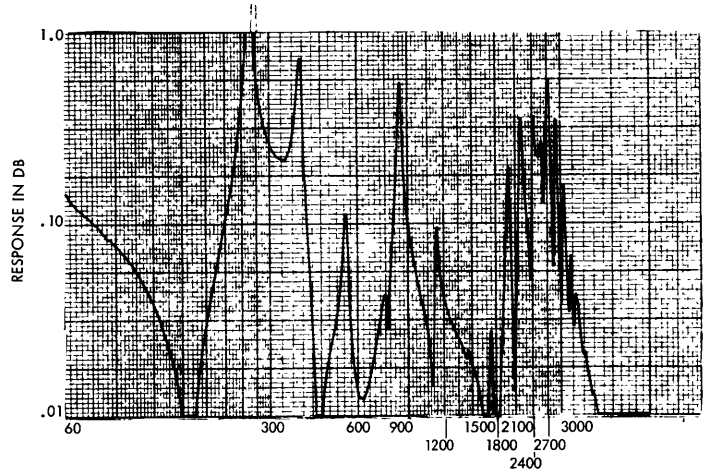

FREQUENCY IN CYCLES PER MINUTE (MECH)

Figure 8.11 System: Rudders and Hull, no damping
Force: Symmetric Rudder Lift
Measure: y-hull Sta. 1.5
S/S_o=0

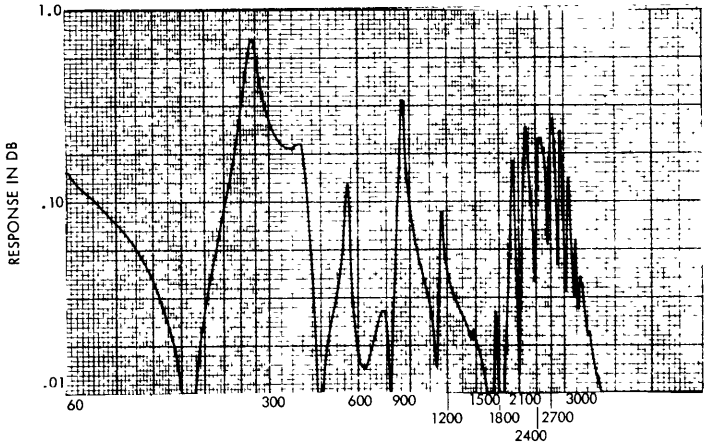

FREQUENCY IN CYCLES PER MINUTE (MECH)

Figure 8.12 System: Rudders and Hull, no damping
Force: Symmetric Rudder Lift
Measure: y-hull Sta. 1.5
S/S_o=0.6

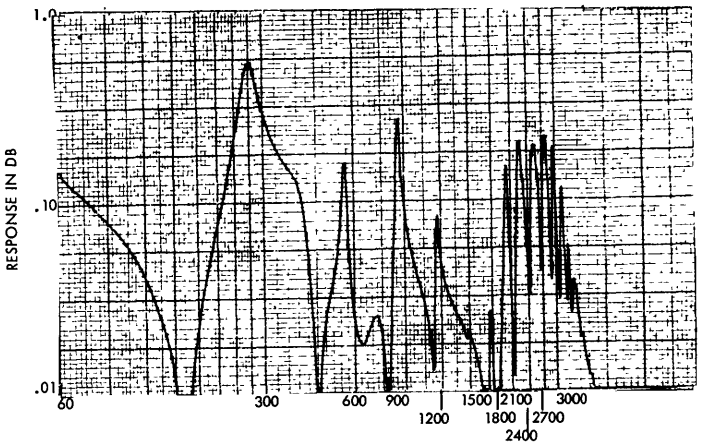

Figure 8.13 System: Rudders and Hull, no damping
Force: Symmetric Rudder Lift
Measure: y-hull Sta. 1.5
S/S_o=1.0

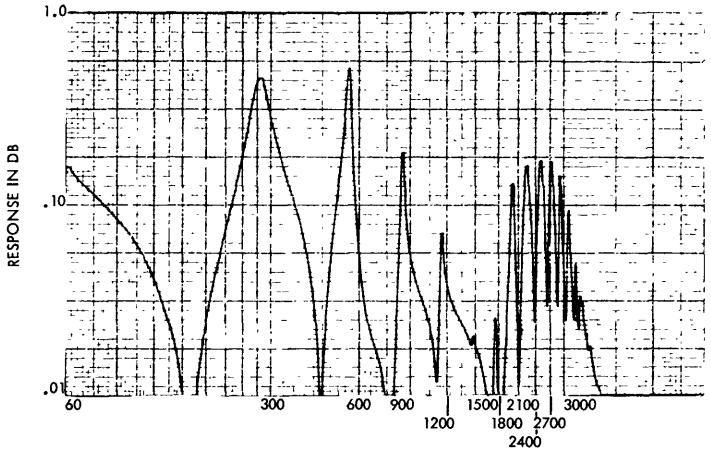

Figure 8.14 System: Rudders and Hull, no damping
Force: Symmetric Rudder Lift
Measure: y-hull Sta. 1.5
S/S_o=1.6

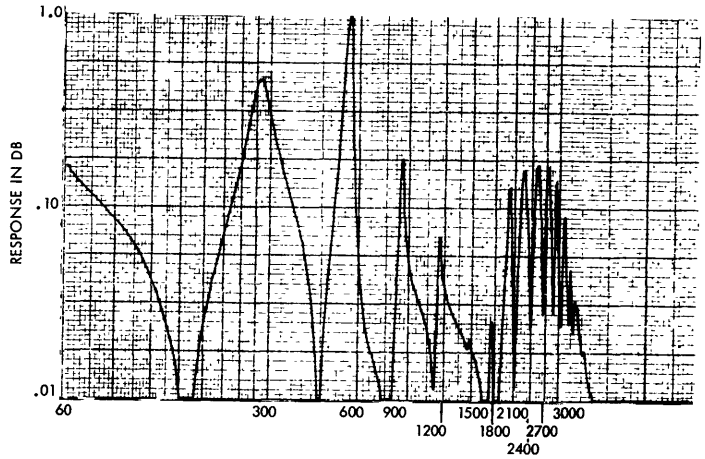

Figure 8.15 System: Rudders and Hull, no damping
Force: Symmetric Rudder Lift
Measure: y-hull Sta. 1.5
S/S_o=1.7

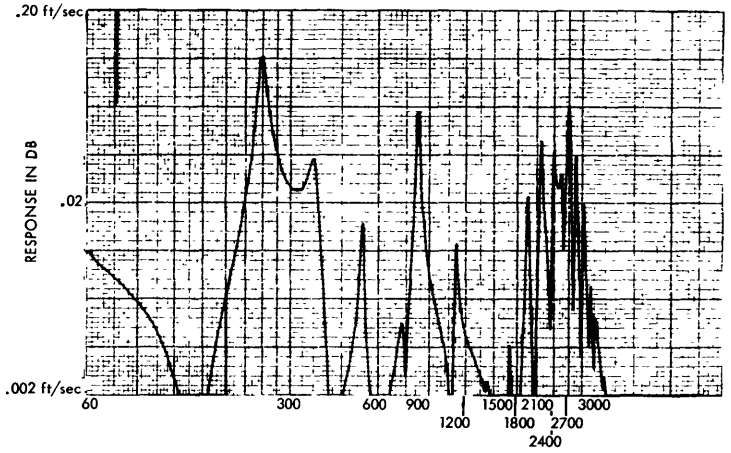

Figure 8.16 System: Rudders and Hull
Force: Symmetric Rudder Lift (1 Ton Apiece)
Measure: y-hull Sta. 1.5
S/S_o=0

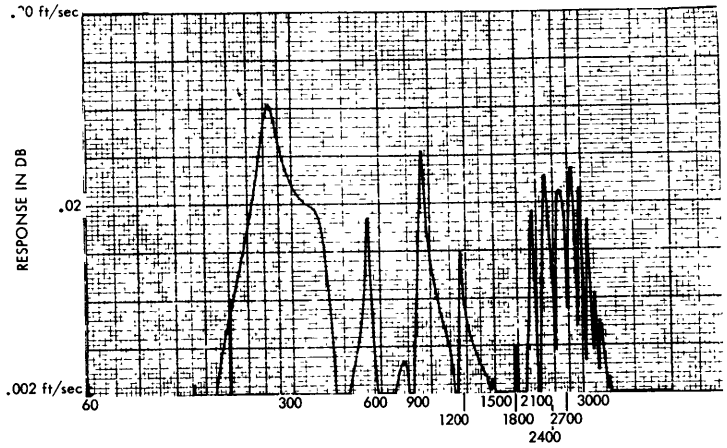

Figure 8.17 System: Rudders and Hull
Force: Symmetric Rudder Lift (1 Ton Apiece)
Measure: y-hull Sta. 1.5
S/S_o=0.6

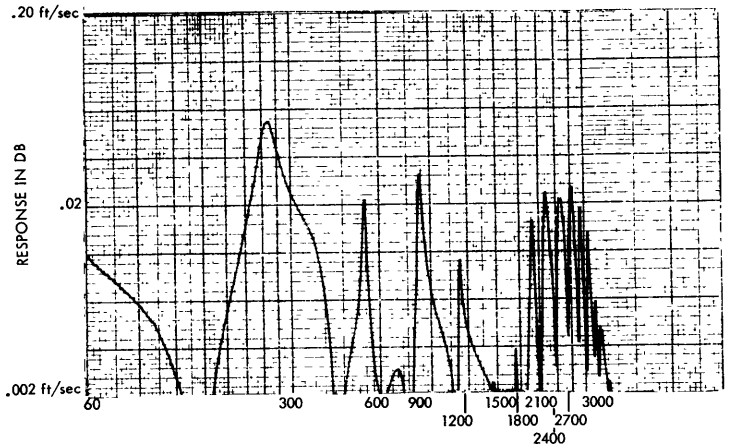

Figure 8.18 System: Rudders and Hull
Force: Symmetric Rudder Lift (1 Ton Apiece)
Measure: y-hull Sta. 1.5
S/S_o=1.0

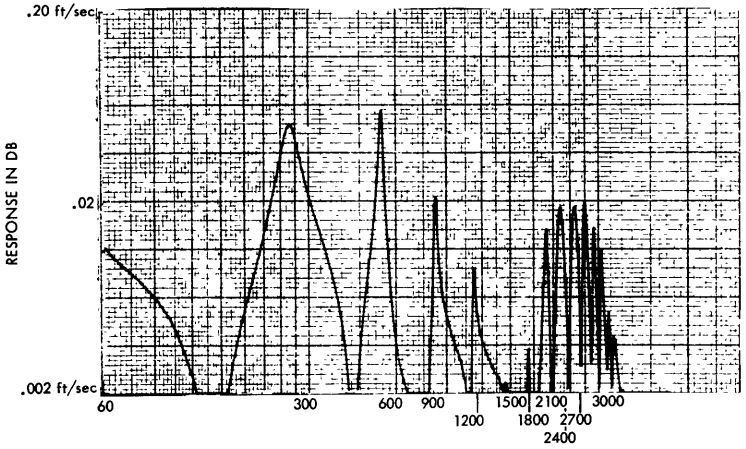

Figure 8.19 System: Rudders and Hull
Force: Symmetric Rudder Lift (1 Ton Apiece)
Measure: y-hull Sta. 1.5
S/S_o=1.6

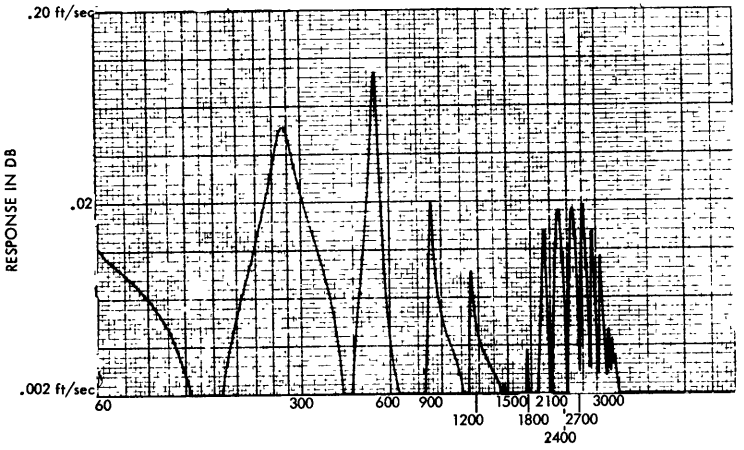

Figure 8.20 System: Rudders and Hull
Force: Symmetric Rudder Lift (1 Ton Apiece)
Measure: y-hull Sta. 1.5
S/S_o=1.7

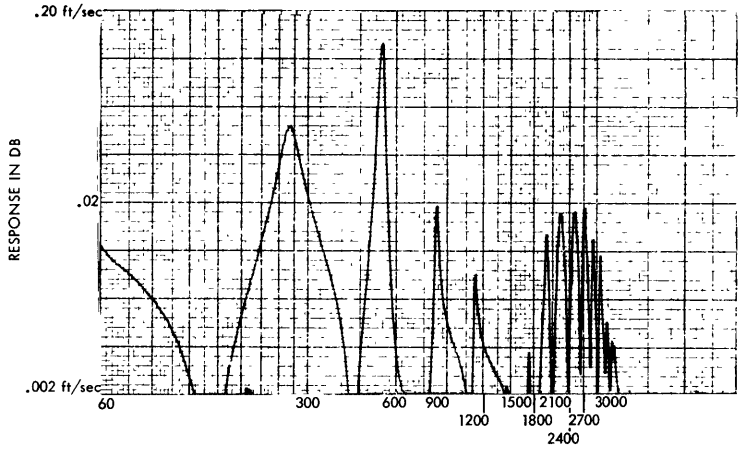

FREQUENCY IN CYCLES PER MINUTE (MECH)

Figure 8.21 System: Rudders and Hull
Force: Symmetric Rudder Lift (1 Ton Apiece)
Measure: y-hull Sta. 1.5
S/S_o=1.75

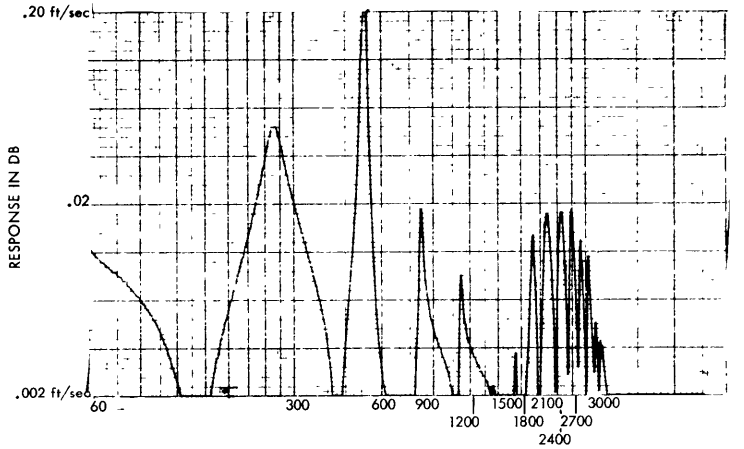

FREQUENCY IN CYCLES PER MINUTE (MECH)

Figure 8.21a System: Rudders and Hull
Force: Symmetric Rudder Lift (1 Ton Apiece)
Measure: y-hull Sta. 1.5
S/S_o=1.80

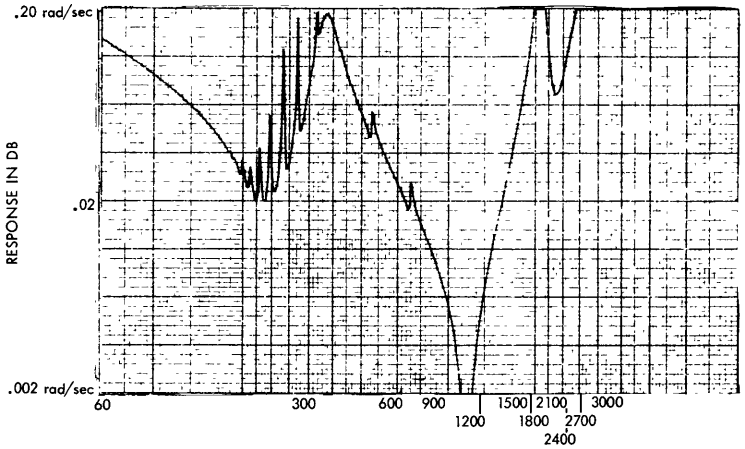

FREQUENCY IN CYCLES PER MINUTE (MECH)

Figure 8.22 System: Rudders and Hull
Force: Symmetric Rudder Lift (1 Ton Apiece)
Measure: γ-upper rudder
S/S_o=1.75

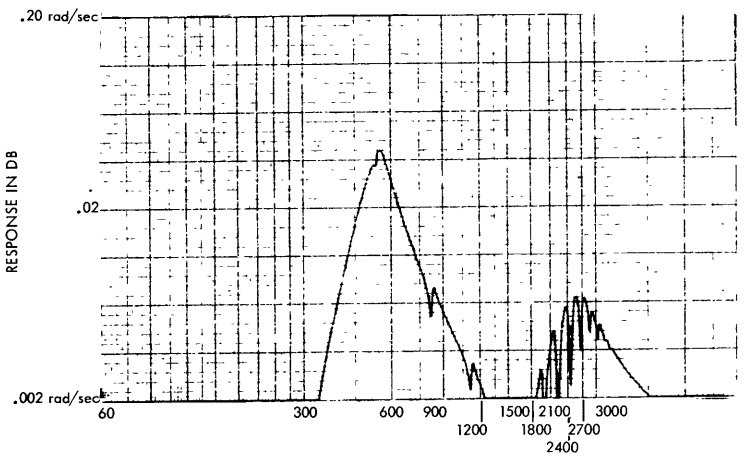

FREQUENCY IN CYCLES PER MINUTE (MECH)

Figure 8.23 System: Rudders and Hull
Force: Symmetric Rudder Lift (1 Ton Apiece)
Measure: γ-upper rudder
S/S_o=1.60

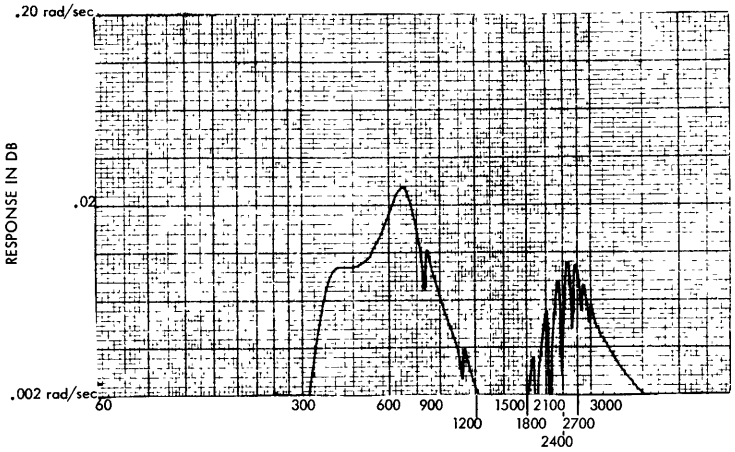

FREQUENCY IN CYCLES PER MINUTE (MECH)

Figure 8.24 System: Rudders and Hull
Force: Symmetric Rudder Lift (1 Ton Apiece)
Measure: γ-upper rudder
S/S_o=1.00

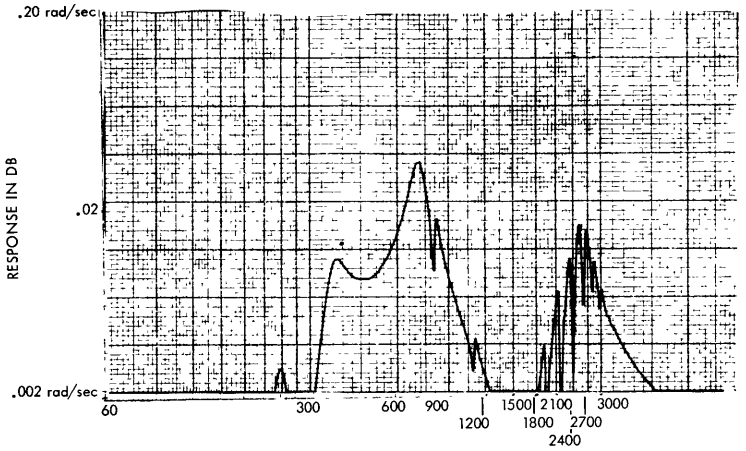

FREQUENCY IN CYCLES PER MINUTE (MECH)

Figure 8.25 System: Rudders and Hull
Force: Symmetric Rudder Lift (1 Ton Apiece)
Measure: γ-upper rudder
S/S_o=0.60

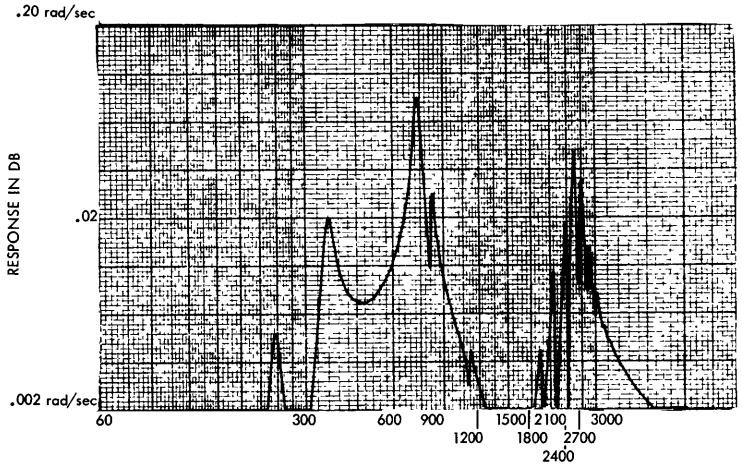

FREQUENCY IN CYCLES PER MINUTE (MECH)

Figure 8.26 System: Rudders and Hull
Force: Symmetric Rudder Lift (1 Ton Apiece)
Measure: γ-upper rudder
S/S_o=0

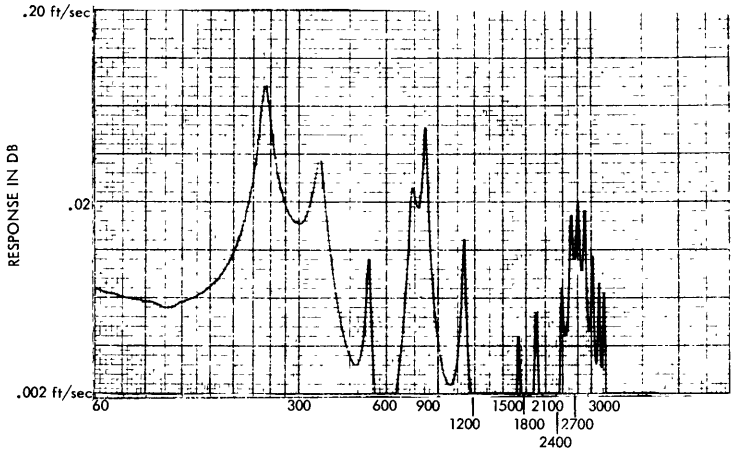

FREQUENCY IN CYCLES PER MINUTE (MECH)

Figure 8.27 System: Rudders and Hull
Force: Symmetric Rudder Lift (1 Ton Apiece)
Measure: y-hull Sta. 18.5
S/S_o=0

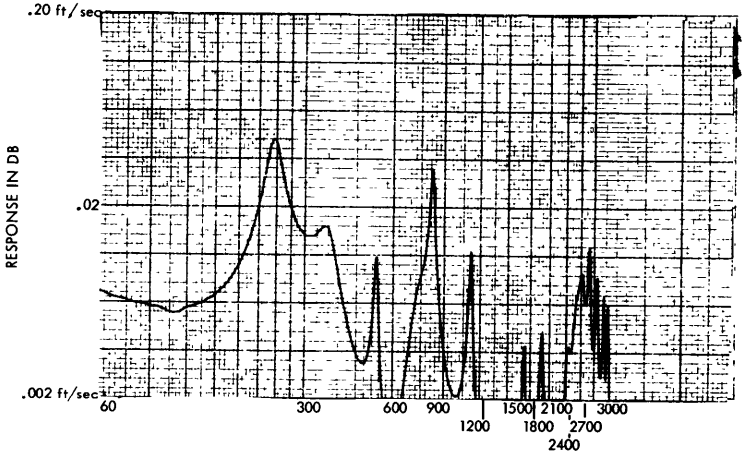

FREQUENCY IN CYCLES PER MINUTE (MECH)

Figure 8.28 System: Rudders and Hull
Force: Symmetric Rudder Lift (1 Ton Apiece)
Measure: y-hull Sta. 18.5
S/S_o=0.60

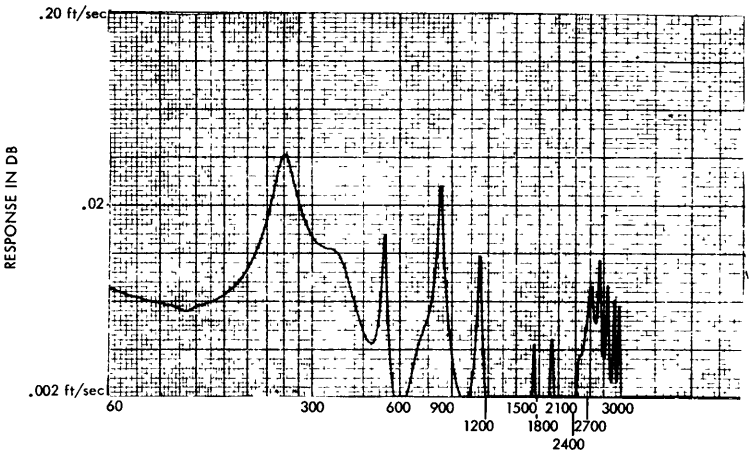

FREQUENCY IN CYCLES PER MINUTE (MECH)

Figure 8.29 System: Rudders and Hull
Force: Symmetric Rudder Lift (1 Ton Apiece)
Measure: y-hull Sta. 18.5
S/S_o=1.00

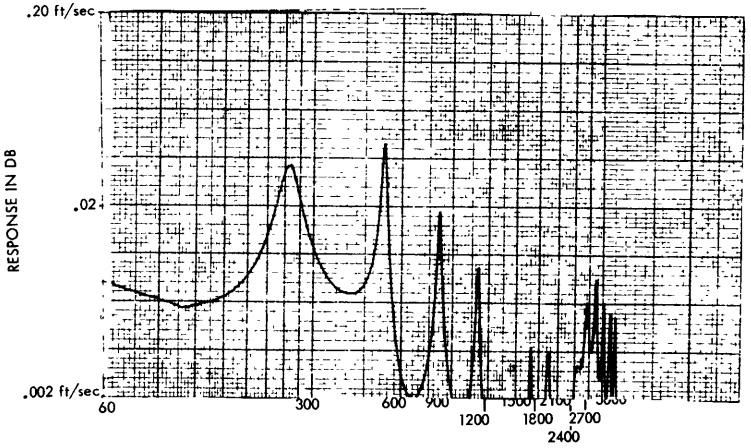

FREQUENCY IN CYCLES PER MINUTE (MECH)

Figure 8.30 System: Rudders and Hull
Force: Symmetric Rudder Lift (1 Ton Apiece)
Measure: y-hull Sta. 18.5
S/S_o=1.60

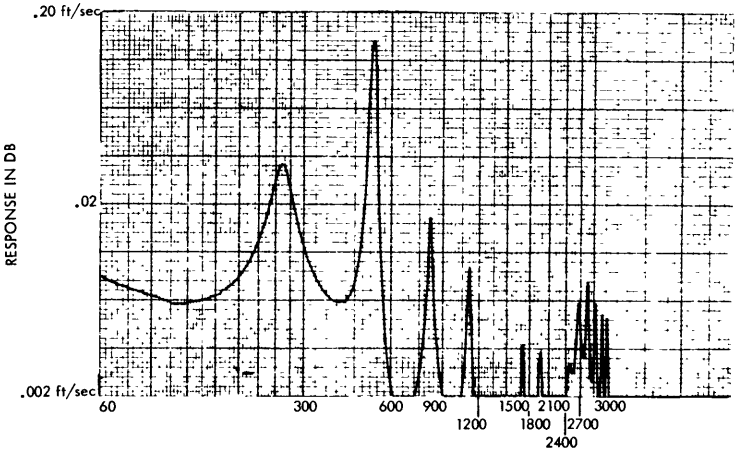

FREQUENCY IN CYCLES PER MINUTE (MECH)

Figure 8.31 System: Rudders and Hull
Force: Symmetric Rudder Lift (1 Ton Apiece)
Measure: y-hull Sta. 18.5
S/S_o=1.80

Figure 9 - Amplitude versus Frequency of Hull; L = +.90

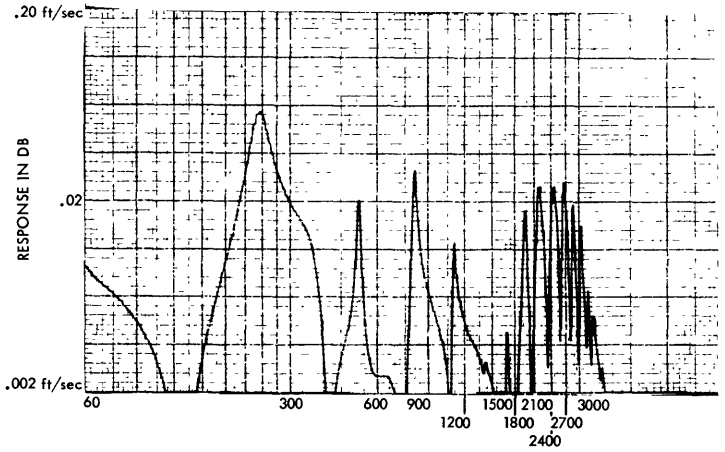

FREQUENCY JN CYCLES PER MINUTE (MECH)

Figure 9.1 System: Hull and Rudders, L=.90
Force: Symmetric Rudder Lift (1 Ton Apiece)
Measure: y-hull Sta. 1.5
S/S_o=1.00

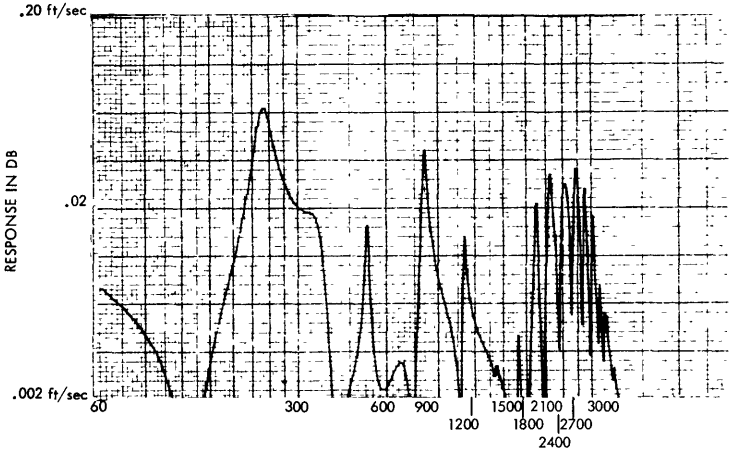

FREQUENCY IN CYCLES PER MINUTE (MECH)

Figure 9.2 System: Hull and Rudders, L=.90
Force: Symmetric Rudder Lift (1 Ton Apiece)
Measure: y-hull Sta. 1.5
S/S_o=0.60

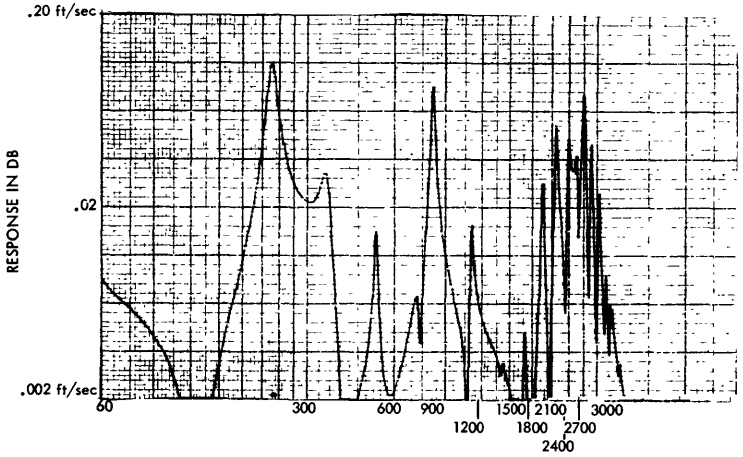

FREQUENCY IN CYCLES PER MINUTE (MECH)

Figure 9.3 System: Hull and Rudders, L=.90
Force: Symmetric Rudder Lift (1 Ton Apiece)
Measure: y-hull Sta. 1.5
S/S_o=0

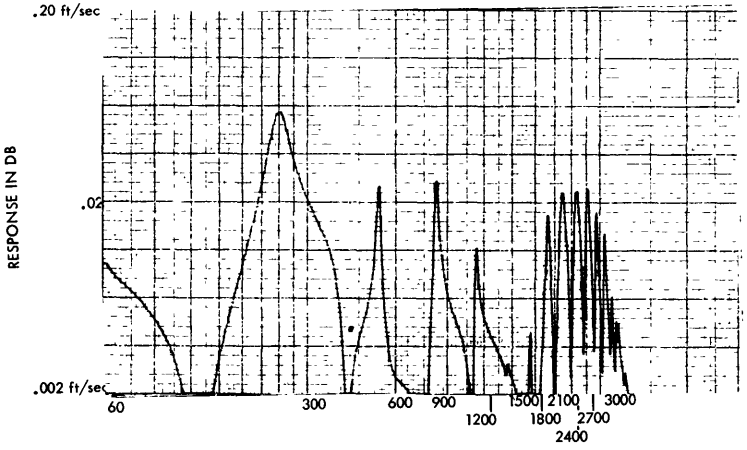

FREQUENCY IN CYCLES PER MINUTE (MECH)

Figure 9.4 System: Hull and Rudders, L=.90
Force: Symmetric Rudder Lift (1 Ton Apiece)
Measure: y-hull Sta. 1.5
S/S_o=1.20

Figure 10 - Amplitude versus Frequency of Hull; L = -.30

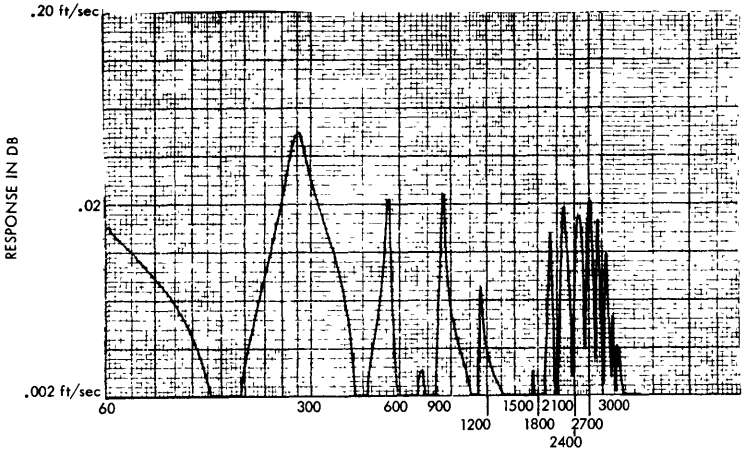

FREQUENCY IN CYCLES PER MINUTE (MECH)

Figure 10.1 System: Hull and Rudders, L=-.30
Force: Symmetric Rudder Lift (1 Ton Apiece)
Measure: y-hull Sta. 1.5
S/S_o=1.40

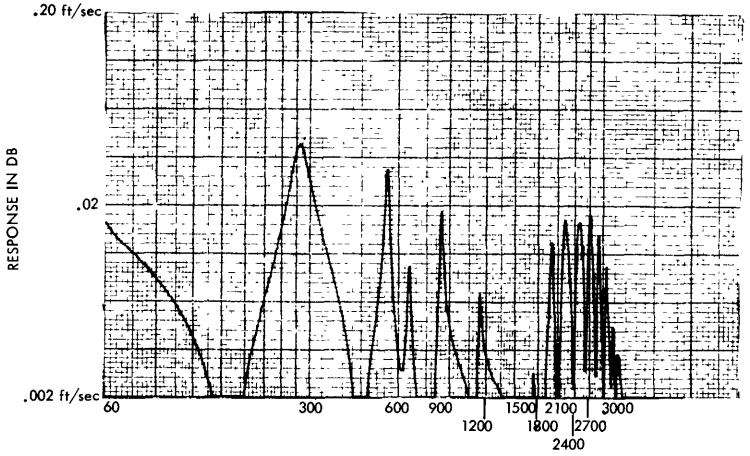

FREQUENCY IN CYCLES PER MINUTE (MECH)

Figure 10.2 System: Hull and Rudders, L=-.30
Force: Symmetric Rudder Lift (1 Ton Apiece)
Measure: y-hull Sta. 1.5
S/S_o=1.90

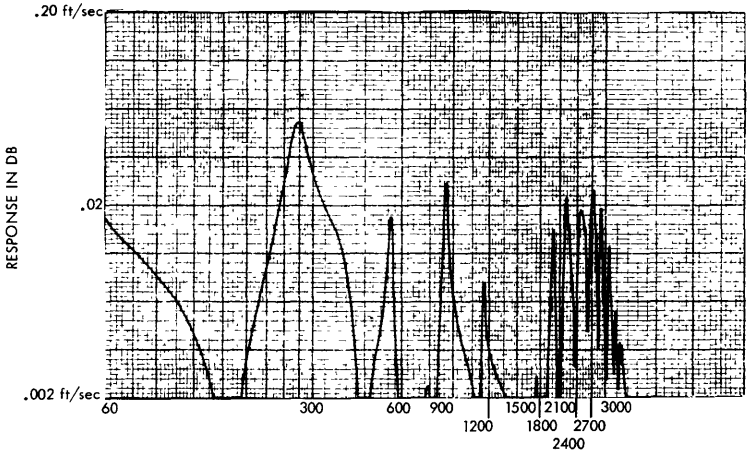

FREQUENCY IN CYCLES PER MINUTE (MECH)

Figure 10.3 System: Hull and Rudders, L=-.30
Force: Symmetric Rudder Lift (1 Ton Apiece)
Measure: y-hull Sta. 1.5
S/S_o=1.00

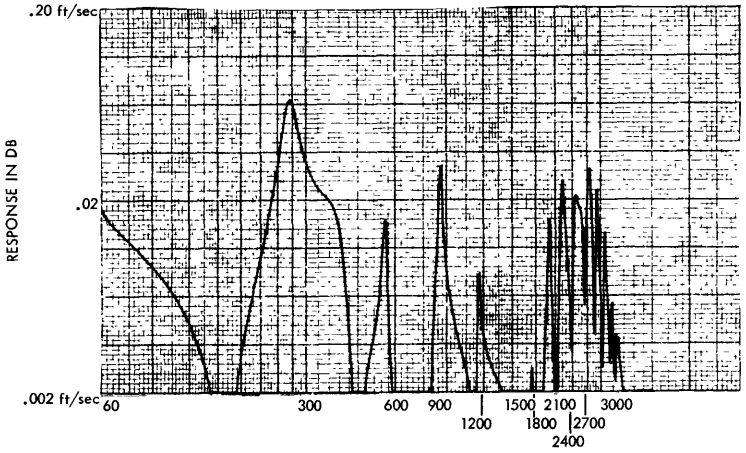

FREQUENCY IN CYCLES PER MINUTE (MECH)

Figure 10.4 System: Hull and Rudders, L=-.30
Force: Symmetric Rudder Lift (1 Ton Apiece)
Measure: y-hull Sta. 1.5
S/S_o=0.6

Figure 11 – Amplitude versus Frequency of Cantilevered Stabilizer and Diving Plane

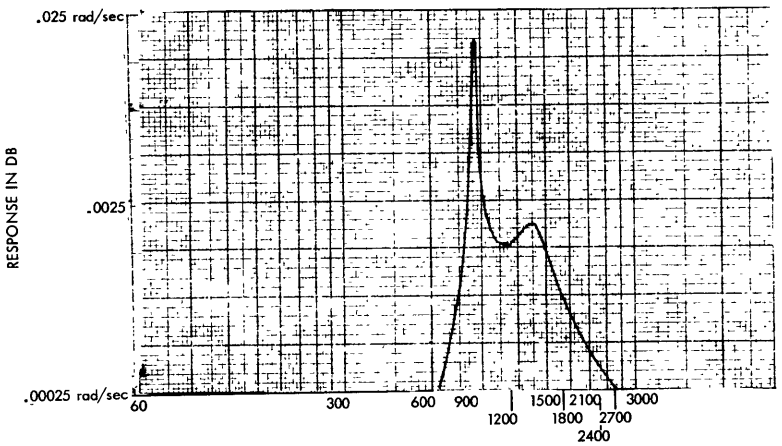

Figure 11.1 System: Cantilevered Stabilizer and Diving Plane
Force: Stabilizer and Diving Plane (1 Ton Total)
Measure: β Diving Plane
S/S_o=0.0

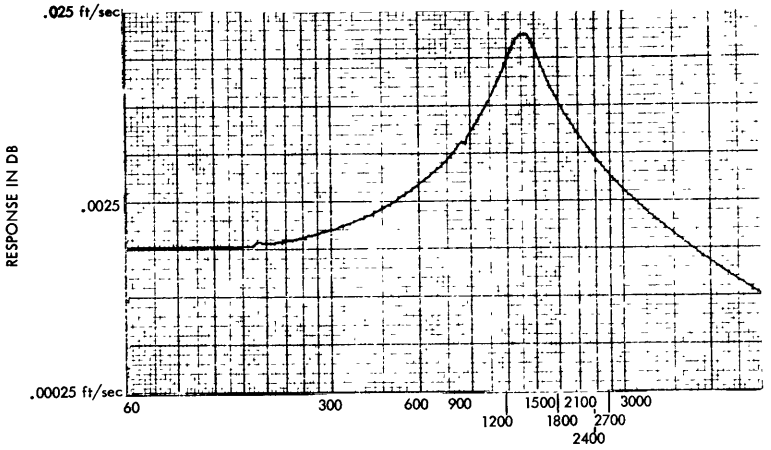

Figure 11.2 System: Cantilevered Stabilizer and Diving Plane
Force: Stabilizer and Diving Plane (1 Ton Total)
Measure: z Stabilizer
S/S_o=0.0

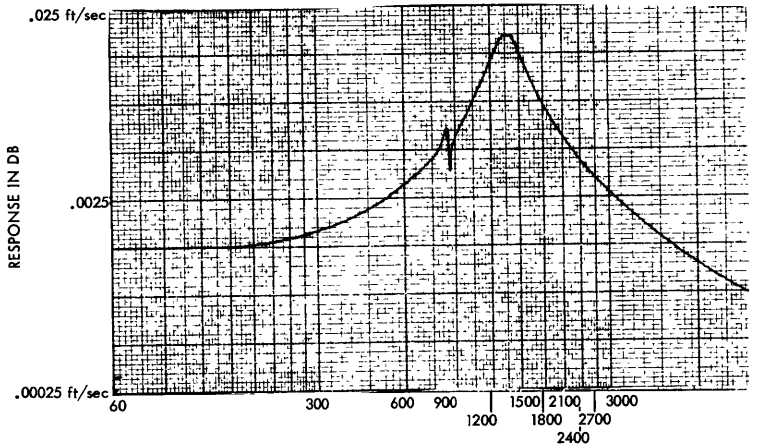

Figure 11.3 System: Cantilevered Stabilizer and Diving Plane
Force: Stabilizer and Diving Plane (1 Ton Total)
Measure: z Diving Plane

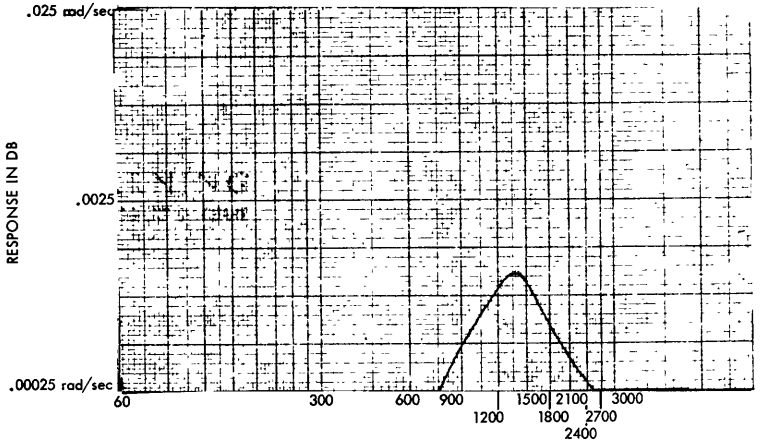

Figure 11.4 System: Cantilevered Stabilizer and Diving Plane
Force: Stabilizer and Diving Plane (1 Ton Total)
Measure: β Diving Plane

Figure 12 - Amplitude versus Frequency of the Basic Submarine

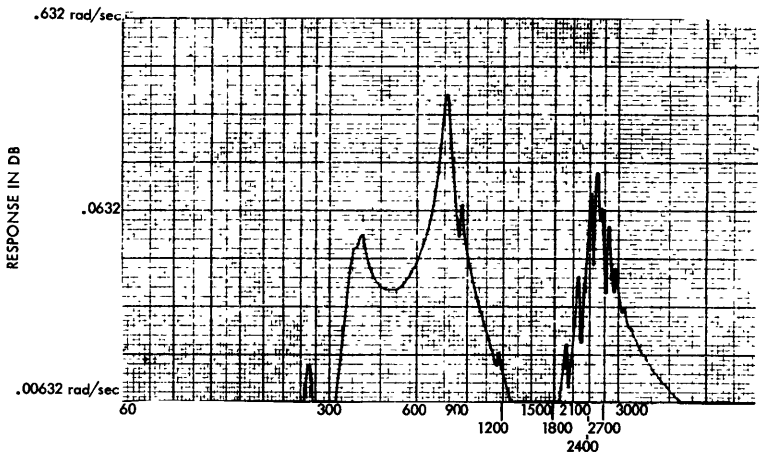

FREQUENCY IN CYCLES PER MINUTE (MECH)

Figure 12.1 System: Basic Submarine
Force: Hydrodynamic Lift on Lower Rudder (1 Ton)
Measure: γ-Lower
$S/S_o=0$

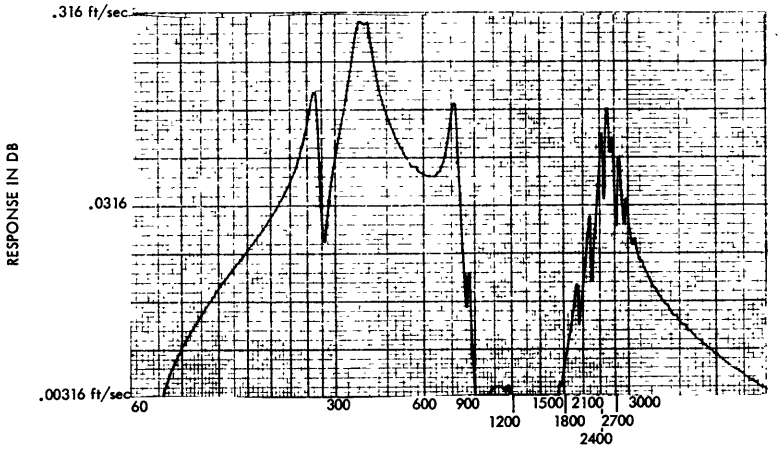

FREQUENCY IN CYCLES PER MINUTE (MECH)

Figure 12.2 System: Basic Submarine
Force: Hydrodynamic Lift on Lower Rudder (1 Ton)
Measure: y-Lower
$S/S_o=0$

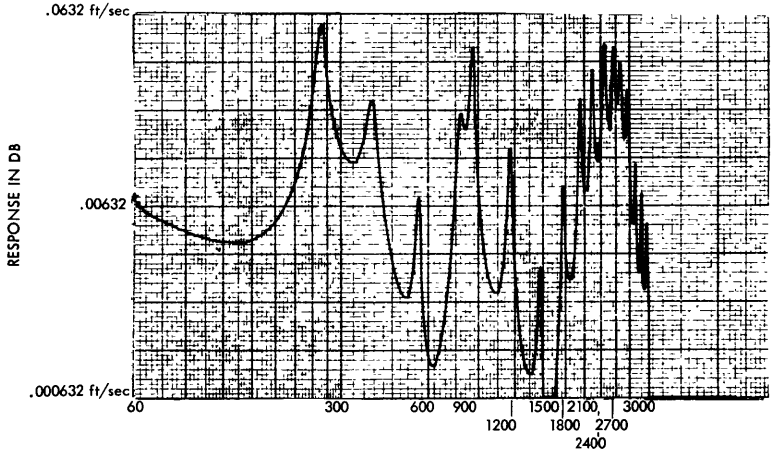

FREQUENCY IN CYCLES PER MINUTE(MECH)

Figure 12.3 System: Basic Submarine
Force: Hydrodynamic Lift on Lower Rudder (1 Ton)
Measure: y-hull 19.5
$S/S_o=0$

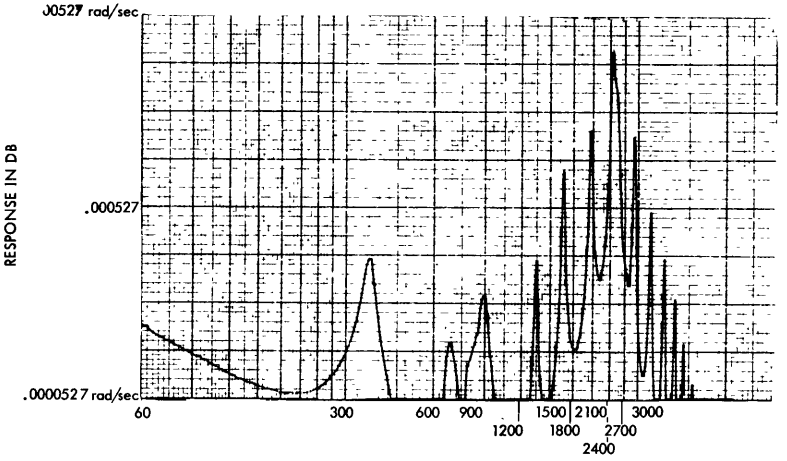

FREQUENCY IN CYCLES PER MINUTE (MECH)

Figure 12.4 System: Basic Submarine
Force: Hydrodynamic Lift on Lower Rudder (1 Ton)
Measure: ∝-Hull 19.5
$S/S_o=0$

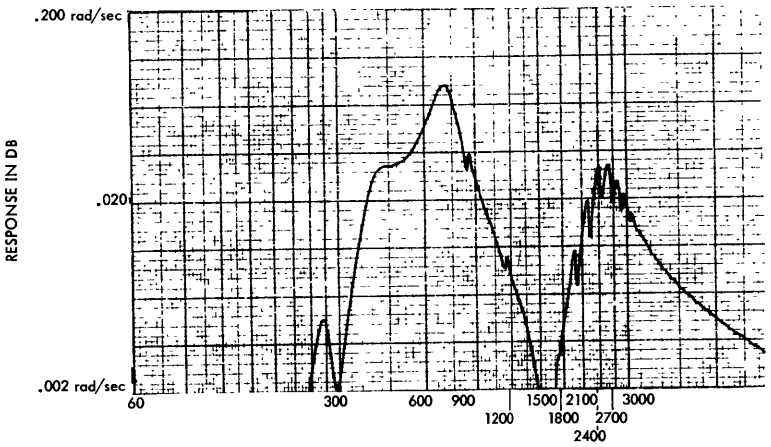

Figure 12.5 System: Basic Submarine
Force: Hydrodynamic Lift on Lower Rudder (1 Ton)
Measure: y-Lower
$S/S_o = 1.0$

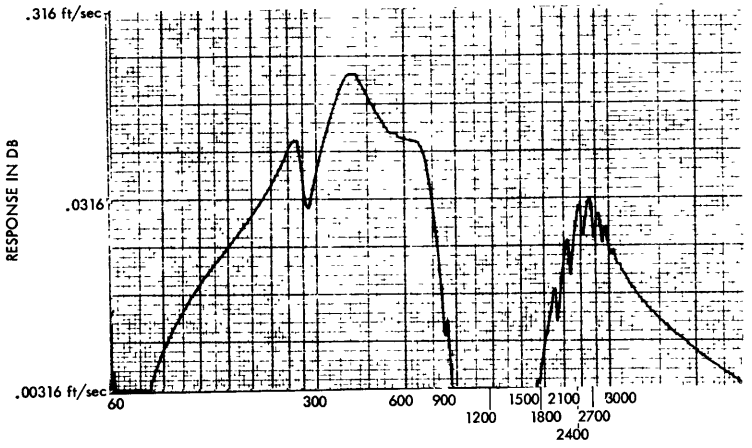

Figure 12.6 System: Basic Submarine
Force: Hydrodynamic Lift on Lower Rudder (1 Ton)
Measure: y-Lower
$S/S_o = 1.0$

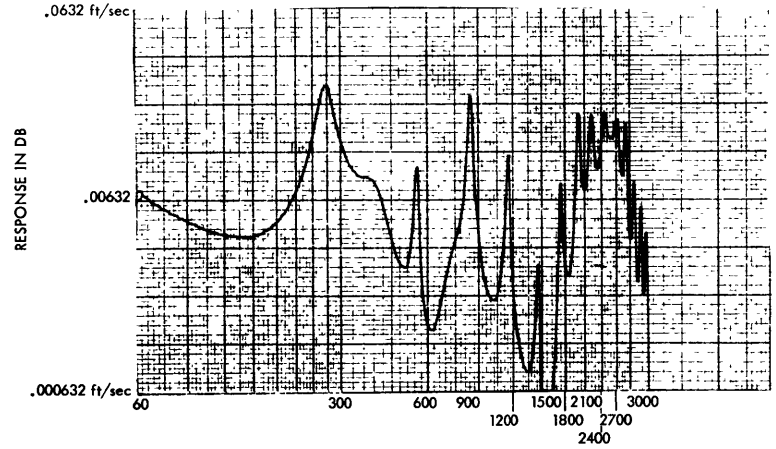

Figure 12.7 System: Basic Submarine
Force: Hydrodynamic Lift on Lower Rudder (1 Ton)
Measure: y-Hull 19.5
$S/S_o = 1.0$

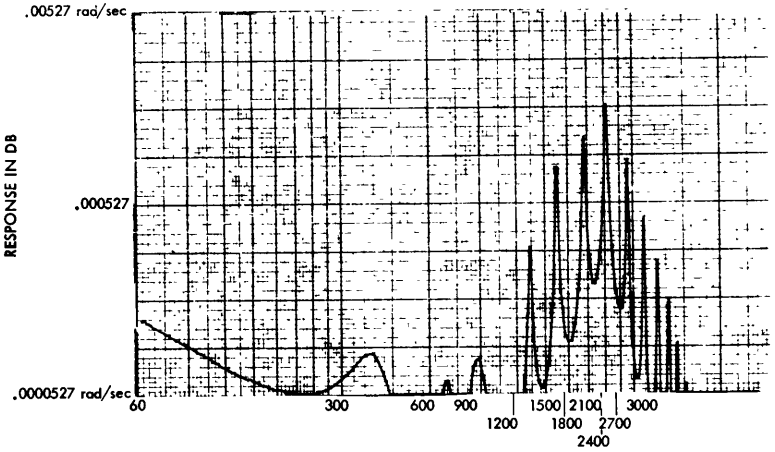

Figure 12.8 System: Basic Submarine
Force: Hydrodynamic Lift on Lower Rudder (1 Ton)
Measure: α - hull 19.5
$S/S_o = 1.0$

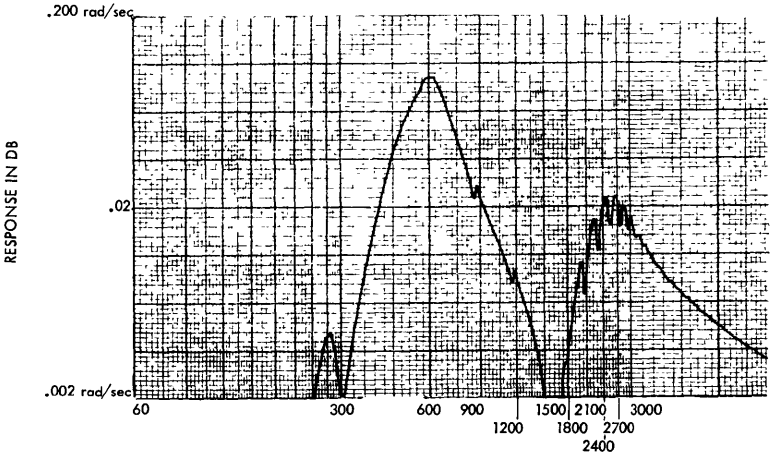

FREQUENCY IN CYCLES PER MINUTE (MECH)

Figure 12.9 System: Basic Submarine
Force: Hydrodynamic Lift on Lower Rudder (1 Ton)
Measure: γ-Lower
S/S_o=1.5

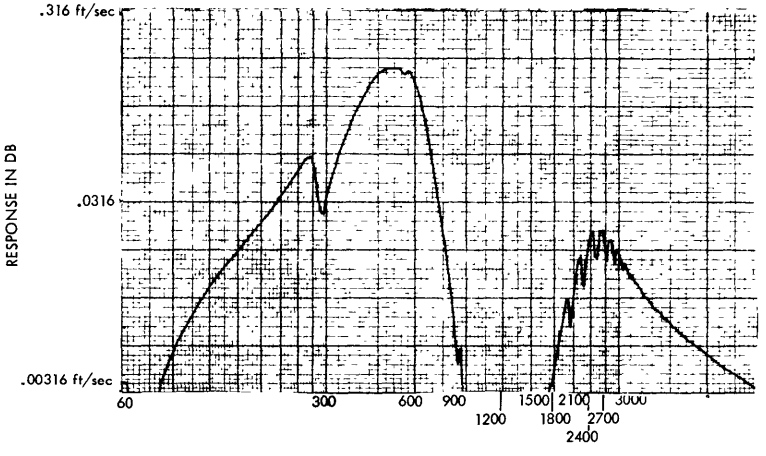

FREQUENCY IN CYCLES PER MINUTE (MECH)

Figure 12.10 System: Basic Submarine
Force: Hydrodynamic Lift on Lower Rudder (1 Ton)
Measure: y-Lower
S/S_o=1.5

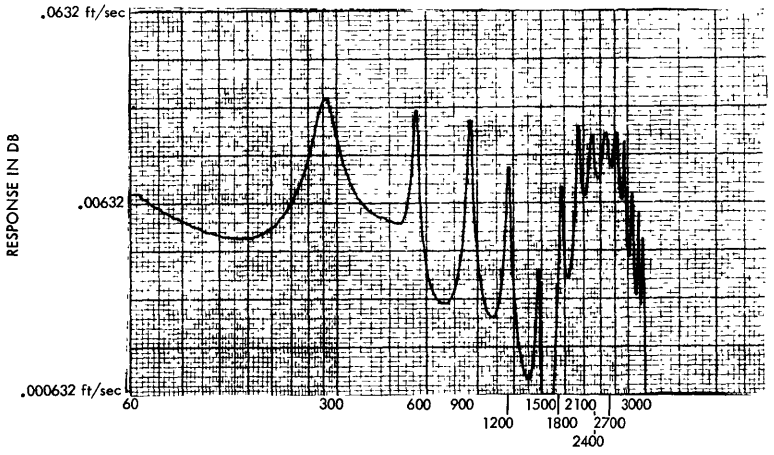

FREQUENCY IN CYCLES PER MINUTE (MECH)

Figure 12.11 System: Basic Submarine
Force: Hydrodynamic Lift on Lower Rudder (1 Ton)
Measure: y-Hull 19.5
S/S_o=1.5

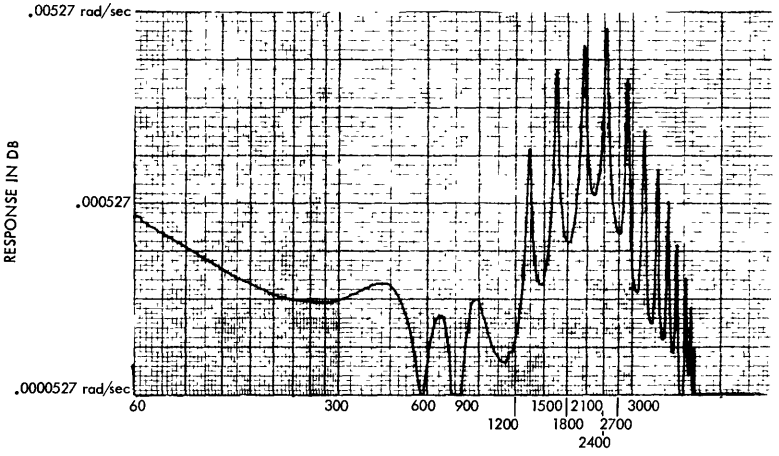

FREQUENCY IN CYCLES PER MINUTE (MECH)

Figure 12.12 System: Basic Submarine
Force: Hydrodynamic Lift on Lower Rudder (1 Ton)
Measure: α-hull 19.5
S/S_o=1.5

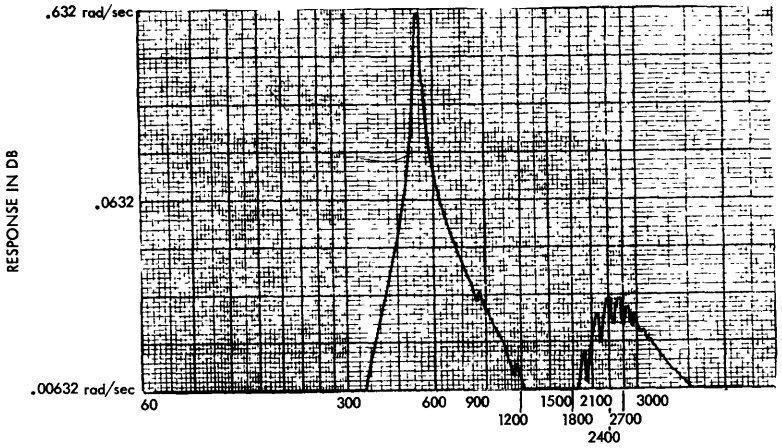

FREQUENCY IN CYCLES PER MINUTE (MECH)

Figure 12.13 System: Basic Submarine
Force: Hydrodynamic Lift on Lower Rudder (1 Ton)
Measure: γ-Lower
S/S_o=1.8

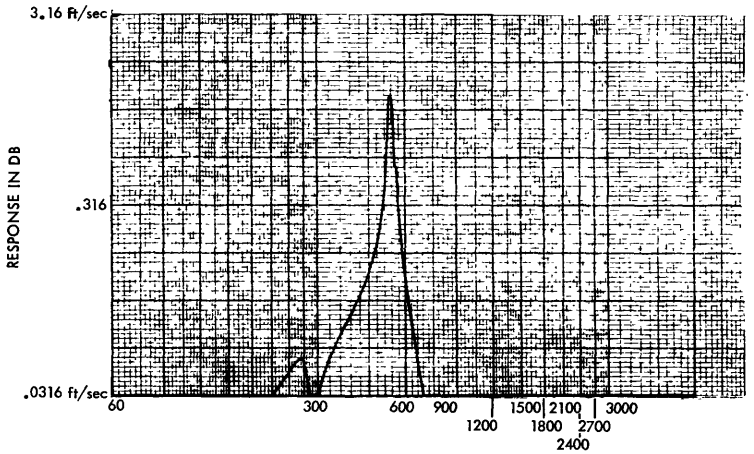

FREQUENCY IN CYCLES PER MINUTE (MECH)

Figure 12.14 System: Basic Submarine
Force: Hydrodynamic Lift on Lower Rudder (1 Ton)
Measure: y-Lower
S/S_o=1.8

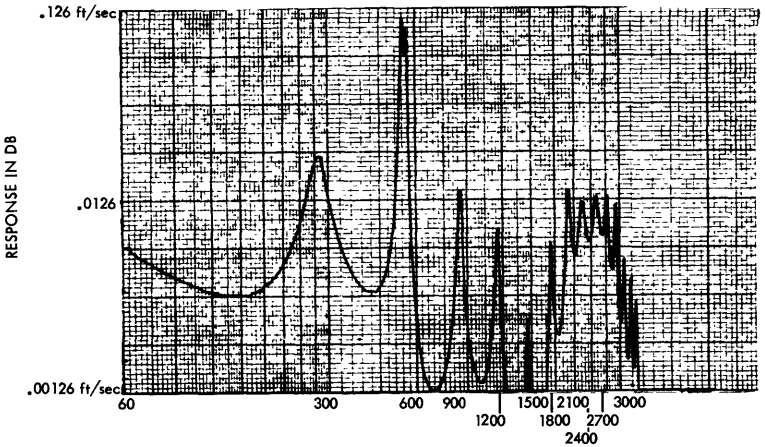

FREQUENCY IN CYCLES PER MINUTE (MECH)

Figure 12.15 System: Basic Submarine
Force: Hydrodynamic Lift on Lower Rudder (1 Ton)
Measure: y-Hull 19.5
S/S_o=1.8

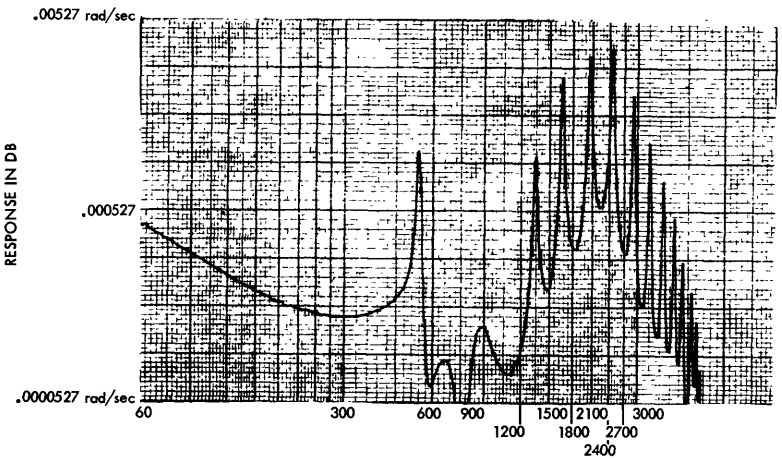

FREQUENCY IN CYCLES PER MINUTE (MECH)

Figure 12.16 System: Basic Submarine
Force: Hydrodynamic Lift on Lower Rudder (1 Ton)
Measure: α-Hull 19.5
S/S_o=1.8

Figure 13 - Amplitude versus Frequency of the Basic Submarine Modified (Appendage Flexibilities Increased)

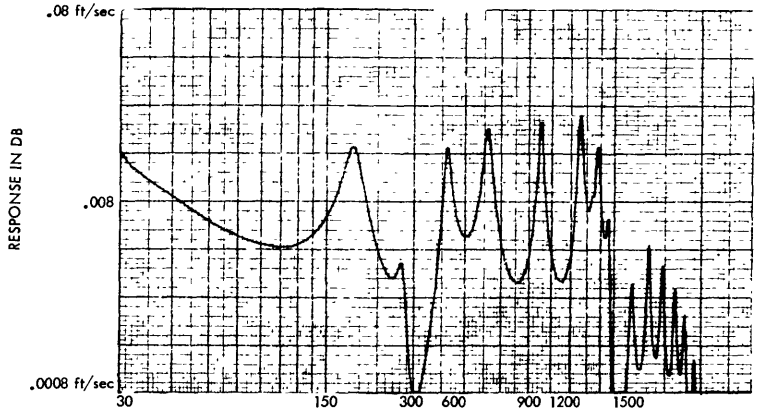

Figure 13.1 System: Basic Hull, 4 times rudder, and diving plane flexibilities
Force: Hydrodynamic Lift on Lower Rudder (1 Ton)
Measure: y-Hull Sta. 19.5
S/S_o=0

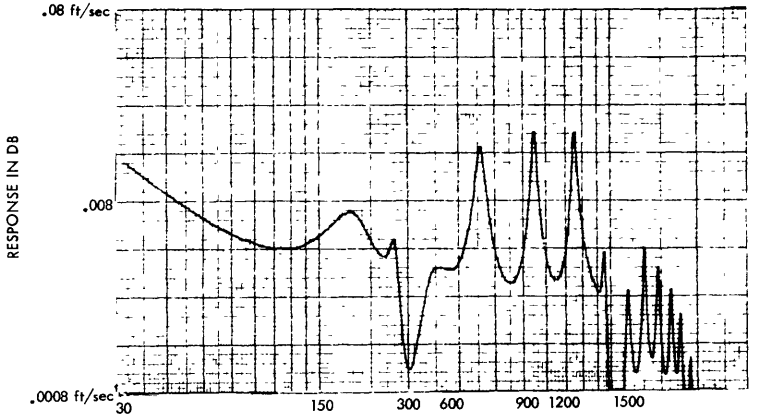

Figure 13.2 System: Basic Hull, 4 times rudder, and diving plane flexibilities
Force: Hydrodynamic Lift on Lower Rudder (1 Ton)
Measure: y-Hull Sta. 19.5
S/S_o=.50

Note: Logarithmic Scale on Abscissae has been multiplied by 15 (See Appendix D)

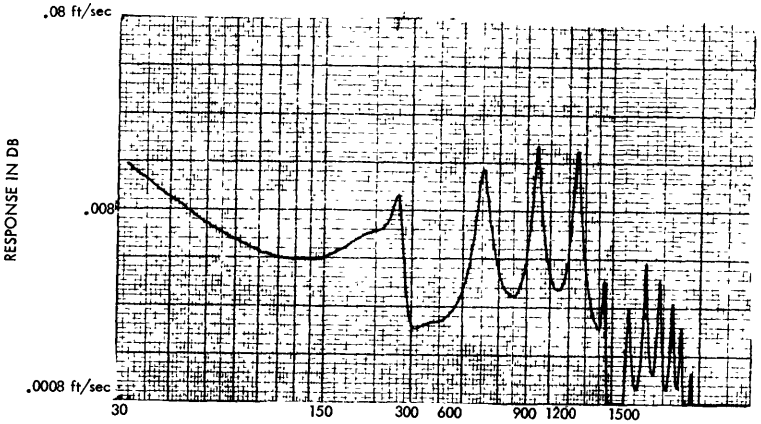

Figure 13.3 System: Basic Hull, 4 times rudder, and diving plane flexibilities
Force: Hydrodynamic Lift on Lower Rudder (1 Ton)
Measure: y-hull Sta. 19.5
S/S_o=0.75

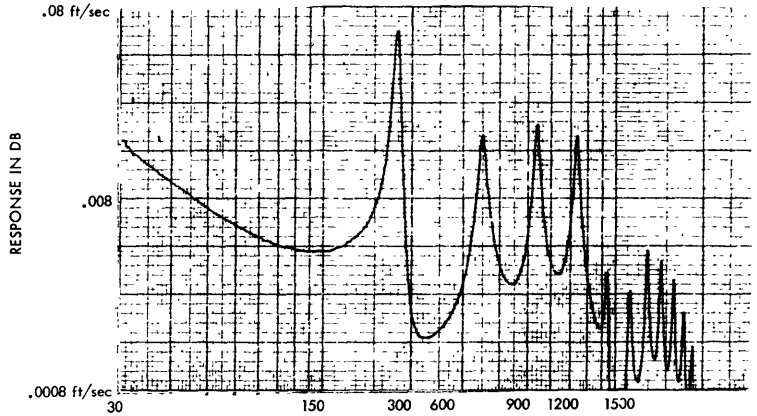

Figure 13.4 System: Basic Hull, 4 times Rudder and diving plane flexibilities
Force: Hydrodynamic Lift on Lower Rudder (1 Ton)
Measure: y-Hull Sta. 19.5
S/S_o=0.90

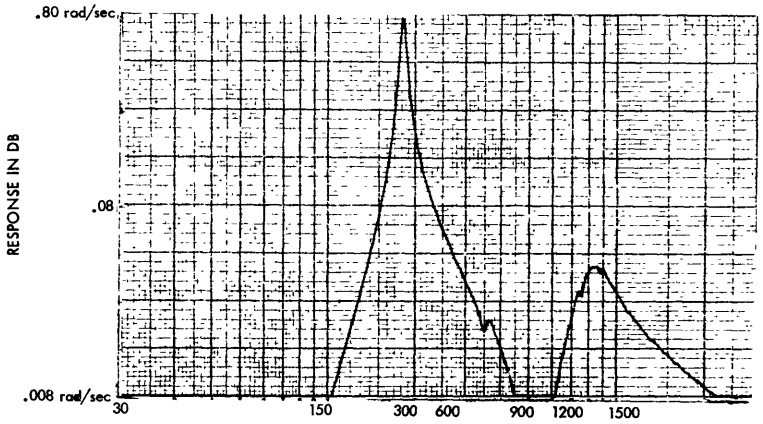

Figure 13.5 System: Basic Hull, 4 times Rudder and diving plane flexibilities
Force: Hydrodynamic Lift on Lower Rudder (1 Ton)
Measure: Y -Lower
S/S_o=0.90

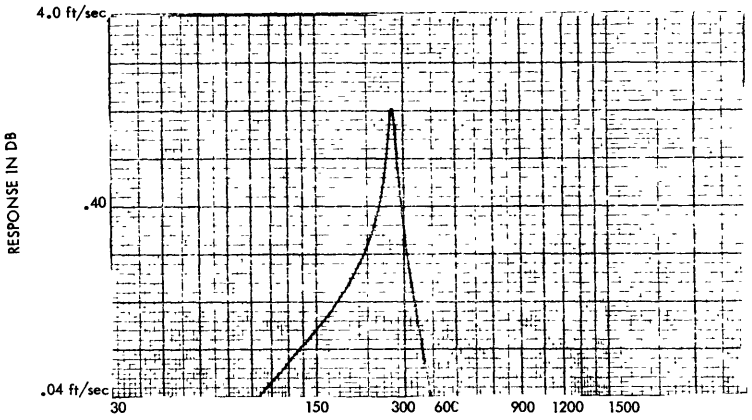

Figure 13.6 System: Basic Hull, 4 times Rudder and diving plane flexibilities
Force: Hydrodynamic Lift on Lower Rudder (1 Ton)
Measure: y-Lower
S/S_o=0.90

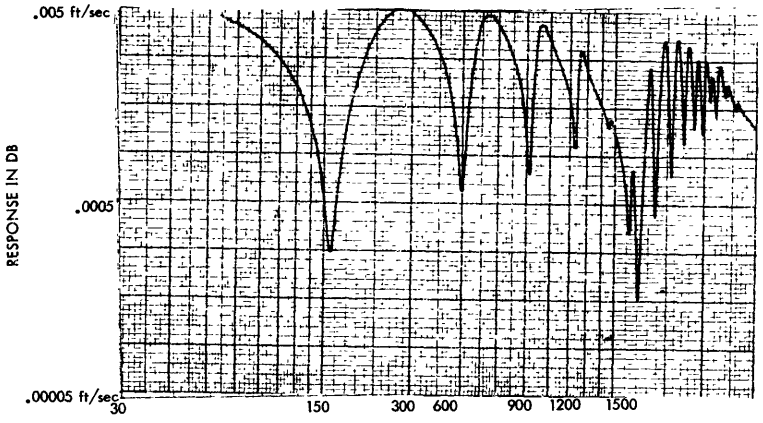

Figure 13.7 System: Hull Only
Force: y-hull Sta. 1.5
Measure: y-hull Sta. 1.5
S/S_o=0

Figure 14 - Amplitude versus Frequency of the Basic Submarine Modified (Mass Coupling Included)

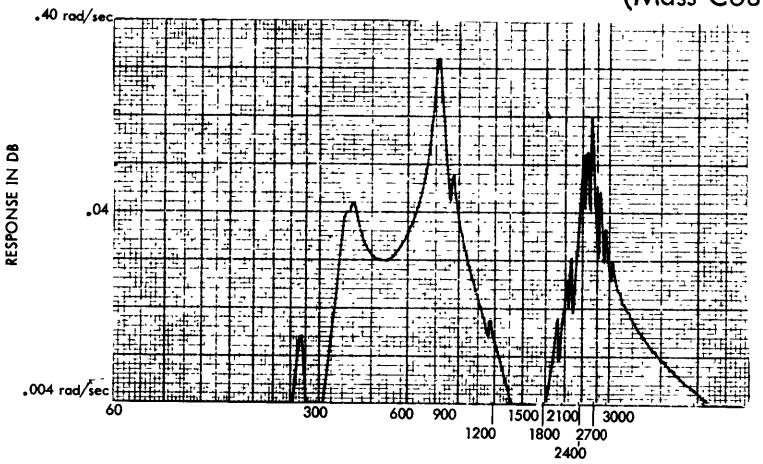

Figure 14.1 System: Submarine with mass coupling
Force: Hydrodynamic Lift on Lower Rudder (1 Ton)
Measure: γ-Lower
S/S_o=0

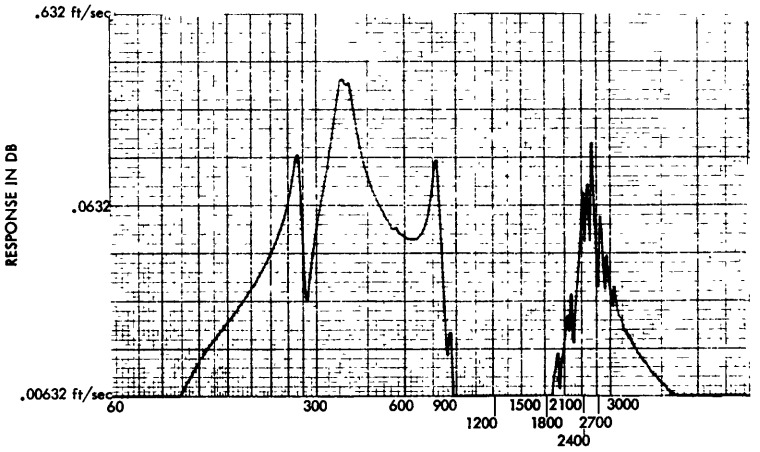

Figure 14.2 System: Submarine with mass coupling
Force: Hydrodynamic Lift on Lower Rudder (1 Ton)
Measure: y-Lower
S/S_o=0

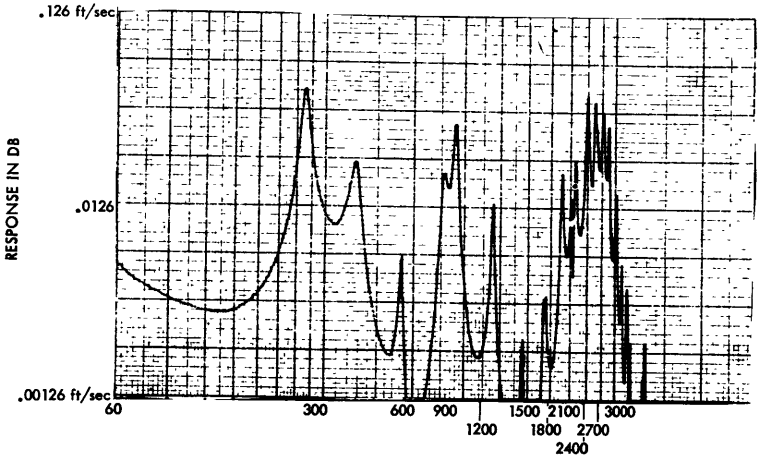

Figure 14.3 System: Submarine with mass coupling
Force: Hydrodynamic Lift on Lower Rudder (1 Ton)
Measure: y-hull 19.5
S/S_o = 0

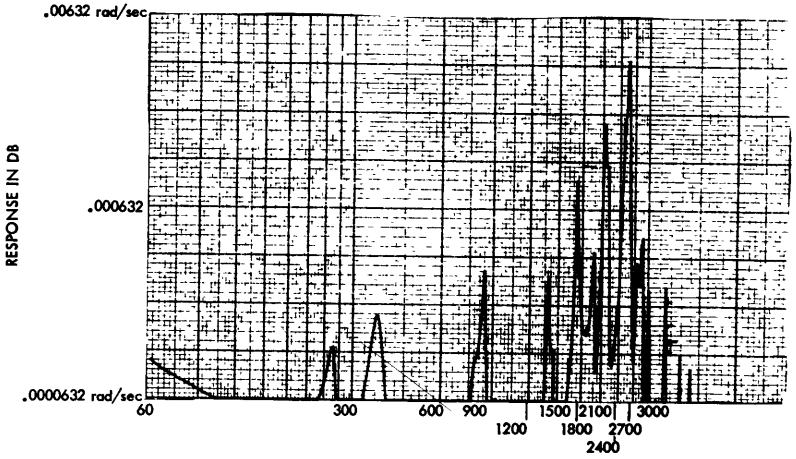

Figure 14.4 System: Submarine with mass coupling
Force: Hydrodynamic Lift on Lower Rudder (1 Ton)
Measure: θ-hull 19.5
S/S_o = 0